Viscous Potential Flow Analysis of Capillary Instability

T. Funada and D.D. Joseph
University of Minnesota
Aug 2001
Draft printed August 18, 2001

Contents

Abstract

Capillary instability of a viscous fluid cylinder of diameter D surrounded by another liquid is determined by a Reynolds number $J = VD\rho_\ell/\mu_\ell$, a viscosity ratio $m = \mu_a/\mu_\ell$ and a density ratio $\ell = \rho_a/\rho_\ell$. Here $V = \gamma/\mu_\ell$ is the capillary collapse velocity based on the more viscous liquid which may be inside or outside the fluid cylinder. Results of linearized analysis based on potential flow of a viscous and inviscid fluid are compared with the unapproximated normal mode analysis of the linearized Navier-Stokes equations. The growth rates for the inviscid fluid are largest, the growth rates of the fully viscous problem are smallest and those of viscous potential flow are between. We find that the results from all three theories converge when J is large with reasonable agreement between viscous potential and fully viscous flow with $J > O(10)$. The convergence results apply to two liquids as well as to liquid and gas.

1 Introduction

Capillary instability of a liquid cylinder of mean radius R leading to capillary collapse can be described as a neckdown due to surface tension γ in which fluid is ejected from the throat of the neck, leading to a smaller neck and greater neckdown capillary force as seen in the diagram in figure 1.1.

The dynamical theory of instability of a long cylindrical column of liquid of radius R under the action of capillary force was given by Rayleigh (1879) [9]

following earlier work by Plateau (1873) [8] who showed that a long cylinder of liquid is unstable to disturbances with wavelengths greater than $2\pi R$. Rayleigh showed that the effect of inertia is such that the wavelength λ corresponding to the mode of maximum instability is $\lambda = 4.51 \times 2R$, exceeding very considerably the circumference of the cylinder. The idea that the wave length associated with fastest growing growth rate would become dominant and be observed in practice was first put forward by Rayleigh (1879) [9]. The analysis of Rayleigh is based on potential flow of an inviscid liquid neglecting the effect of the outside fluid. (Looking forward, we here note that it is possible and useful to do an analysis of this problem based on the potential flow of a viscous fluid).

An attempt to account for viscous effects was made by Rayleigh (1892) [10] again neglecting the effect of the surrounding fluid. One of the effects considered is meant to account for the forward motion of an inviscid fluid with a resistance proportional to velocity. The effect of viscosity is treated in the special case in which the viscosity is so great that inertia may be neglected. He shows that the wavelength for maximum growth is very large, strictly infinite. He says, "... long threads do not tend to divide themselves into drops at mutual distances comparable to with the diameter of the cylinder, but rather to give way by attenuation at few and distant places."

Weber (1931) [12] extended Rayleigh's theory by considering an effect of viscosity and that of surrounding air on the stability of a columnar jet. He showed that viscosity does not alter the value of the cut-off wavenumber predicted by the inviscid theory and that the influence of the ambient air is not significant if the forward speed of the jet is small. Indeed the effects of the ambient fluid, which can be liquid or gas, might be significant in various circumstances. The problem, yet to be considered for liquid jets, is the superposition of Kelvin-Helmholtz and capillary instability.

Tomotika (1935) [11] considered the stability to axisymmetric disturbances of a long cylindrical column of viscous liquid in another viscous fluid under the supposition that the fluids are not driven to move relative to one another. He derived the dispersion relation for the fully viscous case (his (33), our (5.14); he solved it only under the assumption that the time derivative in the equation of motion can be neglected but the time derivative in the kinematic condition is taken into account (his (33)). These approximations were useful in 1935 but are unnecessary in the age of the computer.

The effect of viscosity on the stability of a liquid cylinder when the surrounding fluid is neglected and on a hollow (dynamically passive) cylinder in a viscous liquid was treated briefly by Chandrasekhar (1961) [1]. The parameter $\gamma R\rho_\ell/\mu_\ell^2$ which can be identified as a Reynolds number based on a velocity γ/μ_ℓ, where μ_ℓ is the viscosity of the liquid, appears in the dispersion relation derived there.

Tomotika's problem was studied by Lee and Flumerfelt (1981) [7] without making the approximations used by Tomotika, focusing on the elucidation of various limiting cases defined in terms of three dimensionless parameter, a density ratio, a viscosity ratio and the Ohnesorge number $Oh = \mu_\ell/\sqrt{\rho\gamma D} = J^{1/2}$.

In this paper we treat the general fully viscous problem considered by Tomotika. This problem is resolved completely without approximation and is applied to 14 pairs of viscous fluids. Theories based on viscous and inviscid potential flows are constructed and compared with the fully viscous analysis and with each other.

It is perhaps necessary to call attention to the fact it is neither necessary or desirable to put the viscosities to zero when considering potential flows. The Navier-Stokes equations are satisfied by potential flow; the viscous term is identically zero when the vorticity is zero but the viscous stresses are not zero (Joseph and Liao 1994 [5]). It is not possible to satisfy the no-slip condition at a solid boundary or the continuity of the tangential component of velocity and shear stress at a fluid-fluid boundary when the velocity is given by a potential. The viscous stresses enter into the viscous potential flow analysis of free surface problems through the normal stress balance (5.10) at the interface. Viscous potential flow analysis gives good approximations to fully viscous flows in cases where the shears from the gas flow are negligible; the Rayleigh-Plesset bubble is a potential flow which satisfies the Navier-Stokes equations and all the interface conditions. Joseph, Belanger

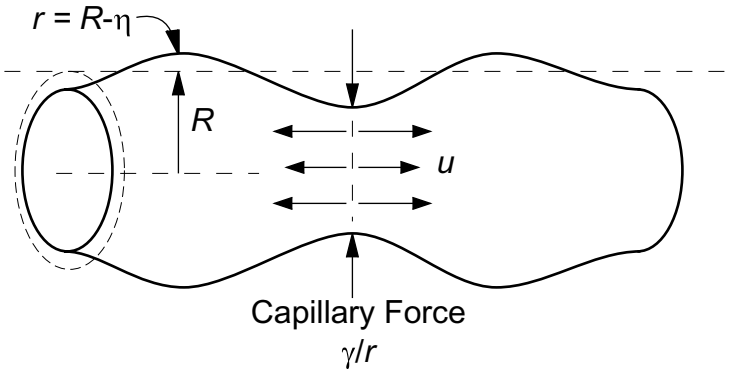

Figure 1.1: *Capillary instability. The force γ/r forces fluid from the throat, decreasing r leading to collapse.*

and Beavers (1999) [4] constructed a viscous potential flow analysis of the Rayleigh-Taylor instability which can scarcely be distinguished from the exact fully viscous analysis. In a recent paper, Funada and Joseph (2001) [2] analyzed Kelvin-Helmholtz instability of a plane gas-liquid layer using viscous potential flow. This problem is not amenable to analysis for the fully viscous case for several reasons identified in their paper. The study leads to unexpected results which appear to agree with experiments.

The present problem of capillary instability can be fully resolved in the fully viscous and potential flow cases and it allows us to precisely identify the limits in which different approximations work well.

2 Basic equations for fully viscous flow (FVF)

Consider the stability of a liquid cylinder of radius R with viscosity μ_ℓ and density ρ_ℓ surrounded by another fluid with viscosity μ_a and density ρ_a under capillary forces generated by interfacial tension γ. Our convention is that $\mu_\ell \geq \mu_a$. In the inverse problem the viscous liquid is outside. The analysis is done in cylindrical coordinates (r, θ, z) and only axisymmetric disturbances independent of θ are considered.

In terms of the cylindrical coordinates (r, θ, z), the velocity (u, v, w) is expressed (for an axisymmetric flow) by the stream function ψ:

$$u = \frac{1}{r}\frac{\partial \psi}{\partial z}, \quad w = -\frac{1}{r}\frac{\partial \psi}{\partial r}. \tag{2.1}$$

The column of fluid ℓ (liquid) is in $0 \leq r < R$ and the fluid a is in $R < r < \infty$. The equations for fluid ℓ are given by

$$\frac{\partial u_\ell}{\partial r} + \frac{u_\ell}{r} + \frac{\partial w_\ell}{\partial z} = 0, \tag{2.2}$$

$$\frac{\partial u_\ell}{\partial t} + u_\ell \frac{\partial u_\ell}{\partial r} + w_\ell \frac{\partial u_\ell}{\partial z} = -\frac{1}{\rho_\ell}\frac{\partial p_\ell}{\partial r} + \nu_\ell \left(\nabla^2 u_\ell - \frac{u_\ell}{r^2}\right), \tag{2.3}$$

$$\frac{\partial w_\ell}{\partial t} + u_\ell \frac{\partial w_\ell}{\partial r} + w_\ell \frac{\partial w_\ell}{\partial z} = -\frac{1}{\rho_\ell}\frac{\partial p_\ell}{\partial z} + \nu_\ell \nabla^2 w_\ell, \tag{2.4}$$

and the equations for fluid a are given by

$$\frac{\partial u_a}{\partial r}+\frac{u_a}{r}+\frac{\partial w_a}{\partial z}=0, \tag{2.5}$$

$$\frac{\partial u_a}{\partial t}+u_a\frac{\partial u_a}{\partial r}+w_a\frac{\partial u_a}{\partial z}=-\frac{1}{\rho_a}\frac{\partial p_a}{\partial r}+\nu_a\left(\nabla^2 u_a-\frac{u_a}{r^2}\right), \tag{2.6}$$

$$\frac{\partial w_a}{\partial t}+u_a\frac{\partial w_a}{\partial r}+w_a\frac{\partial w_a}{\partial z}=-\frac{1}{\rho_a}\frac{\partial p_a}{\partial z}+\nu_a\nabla^2 w_a, \tag{2.7}$$

with the Laplacian:

$$\nabla^2=\frac{\partial^2}{\partial r^2}+\frac{1}{r}\frac{\partial}{\partial r}+\frac{\partial^2}{\partial z^2}. \tag{2.8}$$

The kinematic condition at the interface $r=R+\eta$ is given for each fluid by

$$\frac{\partial \eta}{\partial t}+w_\ell\frac{\partial \eta}{\partial z}=u_\ell \quad\rightarrow\quad \frac{\partial \eta}{\partial t}-\frac{1}{r}\frac{\partial \psi_\ell}{\partial r}\frac{\partial \eta}{\partial z}=\frac{1}{r}\frac{\partial \psi_\ell}{\partial z}, \tag{2.9}$$

$$\frac{\partial \eta}{\partial t}+w_a\frac{\partial \eta}{\partial z}=u_a \quad\rightarrow\quad \frac{\partial \eta}{\partial t}-\frac{1}{r}\frac{\partial \psi_a}{\partial r}\frac{\partial \eta}{\partial z}=\frac{1}{r}\frac{\partial \psi_a}{\partial z}, \tag{2.10}$$

and the normal stress balance at $r=R+\eta$ is given by

$$p_\ell-p_a-\tau_\ell+\tau_a=-\gamma\left\{\frac{\partial^2\eta}{\partial z^2}\left[1+\left(\frac{\partial\eta}{\partial z}\right)^2\right]^{-3/2}-(R+\eta)^{-1}\left[1+\left(\frac{\partial\eta}{\partial z}\right)^2\right]^{-1/2}+\frac{1}{R}\right\}, \tag{2.11}$$

where γ is the surface tension, and τ_ℓ and τ_a denote the normal viscous stresses acting on the interface:

$$\tau_\ell=2\mu_\ell\left[\frac{\partial u_\ell}{\partial r}-\left(\frac{\partial u_\ell}{\partial z}+\frac{\partial w_\ell}{\partial r}\right)\frac{\partial\eta}{\partial z}+\frac{\partial w_\ell}{\partial z}\left(\frac{\partial\eta}{\partial z}\right)^2\right]\left[1+\left(\frac{\partial\eta}{\partial z}\right)^2\right]^{-1}, \tag{2.12}$$

$$\tau_a=2\mu_a\left[\frac{\partial u_a}{\partial r}-\left(\frac{\partial u_a}{\partial z}+\frac{\partial w_a}{\partial r}\right)\frac{\partial\eta}{\partial z}+\frac{\partial w_a}{\partial z}\left(\frac{\partial\eta}{\partial z}\right)^2\right]\left[1+\left(\frac{\partial\eta}{\partial z}\right)^2\right]^{-1}. \tag{2.13}$$

The first term in this right-hand-side remains even if the interface deformation vanishes. It is noted in (2.11) that the pressure in undisturbed state is balanced as

$$\bar{p}_\ell-\bar{p}_a=\gamma\frac{1}{R}, \tag{2.14}$$

which has already been subtracted in (2.11). The pressure in (2.11) is to be evaluated from the equation of motion; (2.3) and (2.6).

The velocity normal to the interface is continuous as

$$\left(u_\ell-w_\ell\frac{\partial\eta}{\partial z}\right)\left[1+\left(\frac{\partial\eta}{\partial z}\right)^2\right]^{-1/2}=\left(u_a-w_a\frac{\partial\eta}{\partial z}\right)\left[1+\left(\frac{\partial\eta}{\partial z}\right)^2\right]^{-1/2}, \tag{2.15}$$

and the velocity tangential to the interface is continuous as

$$\left(u_\ell \frac{\partial \eta}{\partial z} + w_\ell\right)\left[1+\left(\frac{\partial \eta}{\partial z}\right)^2\right]^{-1/2} = \left(u_a \frac{\partial \eta}{\partial z} + w_a\right)\left[1+\left(\frac{\partial \eta}{\partial z}\right)^2\right]^{-1/2}. \tag{2.16}$$

The tangential stress balance is given by

$$\mu_\ell\left[2\frac{\partial u_\ell}{\partial r}\frac{\partial \eta}{\partial z} + \left(\frac{\partial u_\ell}{\partial z}+\frac{\partial w_\ell}{\partial r}\right)\left(1-\left(\frac{\partial \eta}{\partial z}\right)^2\right) - 2\frac{\partial w_\ell}{\partial z}\frac{\partial \eta}{\partial z}\right]\left[1+\left(\frac{\partial \eta}{\partial z}\right)^2\right]^{-1}$$

$$= \mu_a\left[2\frac{\partial u_a}{\partial r}\frac{\partial \eta}{\partial z} + \left(\frac{\partial u_a}{\partial z}+\frac{\partial w_a}{\partial r}\right)\left(1-\left(\frac{\partial \eta}{\partial z}\right)^2\right) - 2\frac{\partial w_a}{\partial z}\frac{\partial \eta}{\partial z}\right]\left[1+\left(\frac{\partial \eta}{\partial z}\right)^2\right]^{-1}. \tag{2.17}$$

The problem for small disturbances in [F] is given by the equations (2.2)–(2.7) and the boundary conditions (2.9)–(2.10), (2.11), (2.15), (2.16), and (2.17).

3 Dimensionless equations for FVF

In terms of the diameter of column D, typical time T, typical velocity $V = D/T$ and typical pressure p_0, we have the normalization:

$$r = D\hat{r}, \quad z = D\hat{z}, \quad t = T\hat{t}, \tag{3.1}$$

$$p = p_0\hat{p}, \quad u = V\hat{u}, \quad w = V\hat{w}, \quad \eta = D\hat{\eta}, \tag{3.2}$$

$$\psi = VD^2\hat{\psi}, \quad R = D\hat{R} \quad \left(\hat{R} = \frac{1}{2}\right), 0 \le m \le \infty. \tag{3.3}$$

The parameters are given by

$$R_e = \frac{VD\rho_\ell}{\mu_\ell} = \frac{VD}{\nu_\ell}, \quad m = \frac{\mu_a}{\mu_\ell}, 0 \le \ell \le \infty \quad \ell = \frac{\rho_a}{\rho_\ell}, 0 \le \ell \le \infty. \tag{3.4}$$

For $p_0 = \gamma/D$ and $V = \gamma/\mu_\ell$, we have the normal stress balance in the undisturbed state

$$\hat{\bar{p}}_\ell - \hat{\bar{p}}_a = 2. \tag{3.5}$$

The dimensionless form of the preceding equations are

$$\frac{\partial \hat{u}_\ell}{\partial \hat{r}} + \frac{\hat{u}_\ell}{\hat{r}} + \frac{\partial \hat{w}_\ell}{\partial \hat{z}} = 0, \tag{3.6}$$

$$R_e\left(\frac{\partial \hat{u}_\ell}{\partial \hat{t}} + \hat{u}_\ell\frac{\partial \hat{u}_\ell}{\partial \hat{r}} + \hat{w}_\ell\frac{\partial \hat{u}_\ell}{\partial \hat{z}}\right) = -\frac{\partial \hat{p}_\ell}{\partial \hat{r}} + \hat{\nabla}^2\hat{u}_\ell - \frac{\hat{u}_\ell}{\hat{r}^2}, \tag{3.7}$$

$$R_e\left(\frac{\partial \hat{w}_\ell}{\partial \hat{t}} + \hat{u}_\ell\frac{\partial \hat{w}_\ell}{\partial \hat{r}} + \hat{w}_\ell\frac{\partial \hat{w}_\ell}{\partial \hat{z}}\right) = -\frac{\partial \hat{p}_\ell}{\partial \hat{z}} + \hat{\nabla}^2\hat{w}_\ell, \tag{3.8}$$

$$\frac{\partial \hat{u}_a}{\partial \hat{r}} + \frac{\hat{u}_a}{\hat{r}} + \frac{\partial \hat{w}_a}{\partial \hat{z}} = 0, \tag{3.9}$$

$$R_e \ell \left(\frac{\partial \hat{u}_a}{\partial \hat{t}} + \hat{u}_a \frac{\partial \hat{u}_a}{\partial \hat{r}} + \hat{w}_a \frac{\partial \hat{u}_a}{\partial \hat{z}} \right) = -\frac{\partial \hat{p}_a}{\partial \hat{r}} + m \left(\hat{\nabla}^2 \hat{u}_a - \frac{\hat{u}_a}{\hat{r}^2} \right), \tag{3.10}$$

$$R_e \ell \left(\frac{\partial \hat{w}_a}{\partial \hat{t}} + \hat{u}_a \frac{\partial \hat{w}_a}{\partial \hat{r}} + \hat{w}_a \frac{\partial \hat{w}_a}{\partial \hat{z}} \right) = -\frac{\partial \hat{p}_a}{\partial \hat{z}} + m \hat{\nabla}^2 \hat{w}_a, \tag{3.11}$$

with

$$\hat{\nabla}^2 = \frac{\partial^2}{\partial \hat{r}^2} + \frac{1}{\hat{r}} \frac{\partial}{\partial \hat{r}} + \frac{\partial^2}{\partial \hat{z}^2}. \tag{3.12}$$

The kinematic condition at $\hat{r} = 1/2 + \hat{\eta}$ is given by

$$\frac{\partial \hat{\eta}}{\partial \hat{t}} + \hat{w}_\ell \frac{\partial \hat{\eta}}{\partial \hat{z}} = \hat{u}_\ell \quad \rightarrow \quad \frac{\partial \hat{\eta}}{\partial \hat{t}} - \frac{1}{\hat{r}} \frac{\partial \hat{\psi}_\ell}{\partial \hat{r}} \frac{\partial \hat{\eta}}{\partial \hat{z}} = \frac{1}{\hat{r}} \frac{\partial \hat{\psi}_\ell}{\partial \hat{z}}, \tag{3.13}$$

$$\frac{\partial \hat{\eta}}{\partial \hat{t}} + \hat{w}_a \frac{\partial \hat{\eta}}{\partial \hat{z}} = \hat{u}_a \quad \rightarrow \quad \frac{\partial \hat{\eta}}{\partial \hat{t}} - \frac{1}{\hat{r}} \frac{\partial \hat{\psi}_a}{\partial \hat{r}} \frac{\partial \hat{\eta}}{\partial \hat{z}} = \frac{1}{\hat{r}} \frac{\partial \hat{\psi}_a}{\partial \hat{z}}. \tag{3.14}$$

The normal stress balance at the interface is given by

$$p_0 \left(\hat{p}_\ell - \hat{p}_a \right) - \mu_\ell \frac{V}{D} \hat{\tau}_\ell + \mu_a \frac{V}{D} \hat{\tau}_a = -\frac{\gamma}{D} \left\{ \frac{\partial^2 \hat{\eta}}{\partial \hat{z}^2} \left[1 + \left(\frac{\partial \hat{\eta}}{\partial \hat{z}} \right)^2 \right]^{-3/2} - \left(\hat{R} + \hat{\eta} \right)^{-1} \left[1 + \left(\frac{\partial \hat{\eta}}{\partial \hat{z}} \right)^2 \right]^{-1/2} + \frac{1}{\hat{R}} \right\}, \tag{3.15}$$

$$\left(\hat{p}_\ell - \hat{p}_a \right) - \hat{\tau}_\ell + m \hat{\tau}_a = - \left\{ \frac{\partial^2 \hat{\eta}}{\partial \hat{z}^2} \left[1 + \left(\frac{\partial \hat{\eta}}{\partial \hat{z}} \right)^2 \right]^{-3/2} - \left(\hat{R} + \hat{\eta} \right)^{-1} \left[1 + \left(\frac{\partial \hat{\eta}}{\partial \hat{z}} \right)^2 \right]^{-1/2} + \frac{1}{\hat{R}} \right\}, \tag{3.16}$$

with the normalized stresses

$$\hat{\tau}_\ell = 2 \left[\frac{\partial \hat{u}_\ell}{\partial \hat{r}} - \left(\frac{\partial \hat{u}_\ell}{\partial \hat{z}} + \frac{\partial \hat{w}_\ell}{\partial \hat{r}} \right) \frac{\partial \hat{\eta}}{\partial \hat{z}} + \frac{\partial \hat{w}_\ell}{\partial \hat{z}} \left(\frac{\partial \hat{\eta}}{\partial \hat{z}} \right)^2 \right] \left[1 + \left(\frac{\partial \hat{\eta}}{\partial \hat{z}} \right)^2 \right]^{-1}, \tag{3.17}$$

$$\hat{\tau}_a = 2 \left[\frac{\partial \hat{u}_a}{\partial \hat{r}} - \left(\frac{\partial \hat{u}_a}{\partial \hat{z}} + \frac{\partial \hat{w}_a}{\partial \hat{r}} \right) \frac{\partial \hat{\eta}}{\partial \hat{z}} + \frac{\partial \hat{w}_a}{\partial \hat{z}} \left(\frac{\partial \hat{\eta}}{\partial \hat{z}} \right)^2 \right] \left[1 + \left(\frac{\partial \hat{\eta}}{\partial \hat{z}} \right)^2 \right]^{-1}. \tag{3.18}$$

The pressure in (3.15) is to be evaluated from the equation of motion; (3.7) and (3.10).

The velocity normal to the interface is continuous as

$$\left(\hat{u}_\ell - \hat{w}_\ell \frac{\partial \hat{\eta}}{\partial \hat{z}} \right) \left[1 + \left(\frac{\partial \hat{\eta}}{\partial \hat{z}} \right)^2 \right]^{-1/2} = \left(\hat{u}_a - \hat{w}_a \frac{\partial \hat{\eta}}{\partial \hat{z}} \right) \left[1 + \left(\frac{\partial \hat{\eta}}{\partial \hat{z}} \right)^2 \right]^{-1/2}, \tag{3.19}$$

and the velocity tangential to the interface is continuous as

$$\left(\hat{u}_\ell \frac{\partial \hat{\eta}}{\partial \hat{z}} + \hat{w}_\ell \right) \left[1 + \left(\frac{\partial \hat{\eta}}{\partial \hat{z}} \right)^2 \right]^{-1/2} = \left(\hat{u}_a \frac{\partial \hat{\eta}}{\partial \hat{z}} + \hat{w}_a \right) \left[1 + \left(\frac{\partial \hat{\eta}}{\partial \hat{z}} \right)^2 \right]^{-1/2}. \tag{3.20}$$

The tangential stress balance is given by

$$\left[2\frac{\partial\hat{u}_\ell}{\partial\hat{r}}\frac{\partial\hat{\eta}}{\partial\hat{z}}+\left(\frac{\partial\hat{u}_\ell}{\partial\hat{z}}+\frac{\partial\hat{w}_\ell}{\partial\hat{r}}\right)\left(1-\left(\frac{\partial\hat{\eta}}{\partial\hat{z}}\right)^2\right)-2\frac{\partial\hat{w}_\ell}{\partial\hat{z}}\frac{\partial\hat{\eta}}{\partial\hat{z}}\right]\left[1+\left(\frac{\partial\hat{\eta}}{\partial\hat{z}}\right)^2\right]^{-1}$$

$$=m\left[2\frac{\partial\hat{u}_a}{\partial\hat{r}}\frac{\partial\hat{\eta}}{\partial\hat{z}}+\left(\frac{\partial\hat{u}_a}{\partial\hat{z}}+\frac{\partial\hat{w}_a}{\partial\hat{r}}\right)\left(1-\left(\frac{\partial\hat{\eta}}{\partial\hat{z}}\right)^2\right)-2\frac{\partial\hat{w}_a}{\partial\hat{z}}\frac{\partial\hat{\eta}}{\partial\hat{z}}\right]\left[1+\left(\frac{\partial\hat{\eta}}{\partial\hat{z}}\right)^2\right]^{-1}. \tag{3.21}$$

4 Dimensionless equations for viscous potential flow (VPF)

The scales used for FVF depend on the viscosity of the fluids and are not appropriate for the case in which the viscosities $\mu_a = \mu_\ell = 0$ or for potential flow generally. To compare VPF and IPF, another choice for scaling the pressure and velocity is appropriate; here we choose the same scales as in (3.1–3.3) except

$$p_0 = \rho_\ell U^2 \tag{4.1}$$

and

$$U = \sqrt{\gamma/D\rho_\ell} \tag{4.2}$$

With these scales, the dimensionless equations for VPF, $\hat{\mathbf{u}} = \hat{\nabla}\hat{\phi}$, $\hat{\nabla}^2\phi = 0$, $\hat{\nabla}^2\hat{\psi} = 0$ which differ from those already given are

$$\left(\frac{\partial\hat{u}_\ell}{\partial\hat{t}}+\hat{u}_\ell\frac{\partial\hat{u}_\ell}{\partial\hat{r}}+\hat{w}_\ell\frac{\partial\hat{u}_\ell}{\partial\hat{z}}\right)=-\frac{\partial\hat{p}_\ell}{\partial\hat{r}} \tag{4.3}$$

$$\left(\frac{\partial\hat{w}_\ell}{\partial\hat{t}}+\hat{u}_\ell\frac{\partial\hat{w}_\ell}{\partial\hat{r}}+\hat{w}_\ell\frac{\partial\hat{w}_\ell}{\partial\hat{z}}\right)=-\frac{\partial\hat{p}_\ell}{\partial\hat{z}} \tag{4.4}$$

and

$$\ell\left(\frac{\partial\hat{u}_a}{\partial\hat{t}}+\hat{u}_a\frac{\partial\hat{u}_a}{\partial\hat{r}}+\hat{w}_a\frac{\partial\hat{u}_a}{\partial\hat{z}}\right)=-\frac{\partial\hat{p}_a}{\partial\hat{r}}\ell\left(\frac{\partial\hat{w}_a}{\partial\hat{t}}+\hat{u}_a\frac{\partial\hat{w}_a}{\partial\hat{r}}+\hat{w}_a\frac{\partial\hat{w}_a}{\partial\hat{z}}\right)=-\frac{\partial\hat{p}_a}{\partial\hat{z}} \tag{4.5}$$

The normal stress balance is given by

$$\hat{p}_\ell-\hat{p}_a-\frac{\hat{\tau}_\ell}{\sqrt{J}}+\frac{m\hat{\tau}_a}{\sqrt{J}}=-\left\{\frac{\partial^2\hat{\eta}}{\partial\hat{z}^2}\left[1+\left(\frac{\partial\hat{\eta}}{\partial\hat{z}}\right)^2\right]^{-\frac{3}{2}}-\left(\frac{1}{2}+\hat{\eta}\right)\left[1+\left(\frac{\partial\hat{\eta}}{\partial\hat{z}}\right)^2\right]^{1/2}+2\right\} \tag{4.6}$$

where $\hat{\tau}_\ell$ and $\hat{\tau}_a$ are defined by (3.10–3.11).

Conditions (3.13)–(3.14) and (3.15)–(3.16) on the tangential component of velocity and stress overdetermine potential flow and they are neglected. Equations (4.3)–(4.6) reduce to IPF when $J \to \infty$.

5 Linear theory of stability for FVF

The system of equations for small disturbances are given by

$$\frac{\partial\hat{u}_\ell}{\partial\hat{r}}+\frac{\hat{u}_\ell}{\hat{r}}+\frac{\partial\hat{w}_\ell}{\partial\hat{z}}=0, \tag{5.1}$$

$$R_e\frac{\partial \hat{u}_\ell}{\partial \hat{t}} = -\frac{\partial \hat{p}_\ell}{\partial \hat{r}} + \hat{\nabla}^2\hat{u}_\ell - \frac{\hat{u}_\ell}{\hat{r}^2}, \quad R_e\frac{\partial \hat{w}_\ell}{\partial \hat{t}} = -\frac{\partial \hat{p}_\ell}{\partial \hat{z}} + \hat{\nabla}^2\hat{w}_\ell, \tag{5.2}$$

$$\frac{\partial \hat{u}_a}{\partial \hat{r}} + \frac{\hat{u}_a}{\hat{r}} + \frac{\partial \hat{w}_a}{\partial \hat{z}} = 0, \tag{5.3}$$

$$R_e\ell\frac{\partial \hat{u}_a}{\partial \hat{t}} = -\frac{\partial \hat{p}_a}{\partial \hat{r}} + m\left(\hat{\nabla}^2\hat{u}_a - \frac{\hat{u}_a}{\hat{r}^2}\right), \quad R_e\ell\frac{\partial \hat{w}_a}{\partial \hat{t}} = -\frac{\partial \hat{p}_a}{\partial \hat{z}} + m\hat{\nabla}^2\hat{w}_a, \tag{5.4}$$

with

$$\hat{\nabla}^2 = \frac{\partial^2}{\partial \hat{r}^2} + \frac{1}{\hat{r}}\frac{\partial}{\partial \hat{r}} + \frac{\partial^2}{\partial \hat{z}^2}. \tag{5.5}$$

The kinematic condition at $\hat{r} = 1/2 + \hat{\eta} \approx 1/2$ is given by

$$\frac{\partial \hat{\eta}}{\partial \hat{t}} = \hat{u}_\ell \quad \rightarrow \quad \frac{\partial \hat{\eta}}{\partial \hat{t}} = \frac{1}{\hat{r}}\frac{\partial \hat{\psi}_\ell}{\partial \hat{z}}, \tag{5.6}$$

$$\frac{\partial \hat{\eta}}{\partial \hat{t}} = \hat{u}_a \quad \rightarrow \quad \frac{\partial \hat{\eta}}{\partial \hat{t}} = \frac{1}{\hat{r}}\frac{\partial \hat{\psi}_a}{\partial \hat{z}}. \tag{5.7}$$

The normal stress balance at the interface is given by

$$(\hat{p}_\ell - \hat{p}_a) - 2\frac{\partial \hat{u}_\ell}{\partial \hat{r}} + 2m\frac{\partial \hat{u}_a}{\partial \hat{r}} = -\left(\frac{\partial^2 \hat{\eta}}{\partial \hat{z}^2} + \frac{\hat{\eta}}{\hat{R}^2}\right). \tag{5.8}$$

The velocity normal to the interface and the velocity tangential to the interface are continuous as

$$\hat{u}_\ell = \hat{u}_a, \quad \hat{w}_\ell = \hat{w}_a. \tag{5.9}$$

The tangential stress balance is given by

$$\left(\frac{\partial \hat{u}_\ell}{\partial \hat{z}} + \frac{\partial \hat{w}_\ell}{\partial \hat{r}}\right) = m\left(\frac{\partial \hat{u}_a}{\partial \hat{z}} + \frac{\partial \hat{w}_a}{\partial \hat{r}}\right). \tag{5.10}$$

The solutions for small disturbances may take the following form:

$$\psi_\ell = [A_1 r I_1(kr) + A_2 r I_1(k_\ell r)]\exp(\sigma t + \imath k z) + c.c., \tag{5.11}$$

$$\psi_a = [B_1 r K_1(kr) + B_2 r K_1(k_a r)]\exp(\sigma t + \imath k z) + c.c., \tag{5.12}$$

$$\eta = H\exp(\sigma t + \imath k z) + c.c., \tag{5.13}$$

for which the solvability condition is given as the dispersion relation of σ:

$$\begin{vmatrix} I_1(kR) & I_1(k_\ell R) & K_1(kR) & K_1(k_a R) \\ kI_0(kR) & k_\ell I_0(k_\ell R) & -kK_0(kR) & -k_a K_0(k_a R) \\ 2\mu_\ell k^2 I_1(kR) & \mu_\ell\left(k^2 + k_\ell^2\right) I_1(k_\ell R) & 2\mu_a k^2 K_1(kR) & \mu_a\left(k^2 + k_a^2\right) K_1(k_a R) \\ F_1 & F_2 & F_3 & F_4 \end{vmatrix} = 0, \tag{5.14}$$

where

$$F_1 = \imath\sigma\rho_\ell I_0(kR) + 2\imath\mu_\ell k^2\left(\frac{\mathrm{d}I_1(kR)}{\mathrm{d}(kR)}\right) - \gamma\left(\frac{1}{R^2} - k^2\right)\imath\frac{k}{\sigma}I_1(kR), \tag{5.15}$$

$$F_2 = 2\imath\mu_\ell k k_\ell\left(\frac{\mathrm{d}I_1(k_\ell R)}{\mathrm{d}(k_\ell R)}\right) - \gamma\left(\frac{1}{R^2} - k^2\right)\imath\frac{k}{\sigma}I_1(k_\ell R), \tag{5.16}$$

$$F_3 = -\imath\sigma\rho_a K_0(kR) + 2\imath\mu_a k^2\left(\frac{\mathrm{d}K_1(kR)}{\mathrm{d}(kR)}\right), \quad F_4 = 2\imath\mu_a k k_a\left(\frac{\mathrm{d}K_1(k_a R)}{\mathrm{d}(k_a R)}\right), \tag{5.17}$$

with

$$k_\ell = \sqrt{k^2 + \frac{\sigma}{\nu_\ell}}, \quad k_a = \sqrt{k^2 + \frac{\sigma}{\nu_a}}. \tag{5.18}$$

The solutions in dimensionless form are given by

$$\hat{\psi}_\ell = \left[\hat{A}_1\hat{r}I_1(\hat{k}\hat{r}) + \hat{A}_2\hat{r}I_1(\hat{k}_\ell\hat{r})\right]\exp(\hat{\sigma}\hat{t} + \imath\hat{k}\hat{z}) + c.c., \tag{5.19}$$

$$\hat{\psi}_a = \left[\hat{B}_1\hat{r}K_1(\hat{k}\hat{r}) + \hat{B}_2\hat{r}K_1(\hat{k}_a\hat{r})\right]\exp(\hat{\sigma}\hat{t} + \imath\hat{k}\hat{z}) + c.c., \tag{5.20}$$

$$\hat{\eta} = \hat{H}\exp(\hat{\sigma}\hat{t} + \imath\hat{k}\hat{z}) + c.c., \tag{5.21}$$

for which the solvability condition is given as the dispersion relation:

$$\begin{vmatrix} I_1(\hat{k}\hat{R}) & I_1(\hat{k}_\ell\hat{R}) & K_1(\hat{k}\hat{R}) & K_1(\hat{k}_a\hat{R}) \\ \hat{k}I_0(\hat{k}\hat{R}) & \hat{k}_\ell I_0(\hat{k}_\ell\hat{R}) & -\hat{k}K_0(\hat{k}\hat{R}) & -\hat{k}_a K_0(\hat{k}_a\hat{R}) \\ 2\hat{k}^2 I_1(\hat{k}\hat{R}) & \left(\hat{k}^2 + \hat{k}_\ell^2\right)I_1(\hat{k}_\ell\hat{R}) & 2m\hat{k}^2 K_1(\hat{k}\hat{R}) & m\left(\hat{k}^2 + \hat{k}_a^2\right)K_1(\hat{k}_a\hat{R}) \\ \hat{F}_1 & \hat{F}_2 & \hat{F}_3 & \hat{F}_4 \end{vmatrix} = 0, \tag{5.22}$$

where

$$\hat{F}_1 = \imath R_e\hat{\sigma}I_0(\hat{k}\hat{R}) + 2\imath\hat{k}^2\left(\frac{\mathrm{d}I_1(\hat{k}\hat{R})}{\mathrm{d}(\hat{k}\hat{R})}\right) - \left(\frac{1}{\hat{R}^2} - \hat{k}^2\right)\imath\frac{\hat{k}}{\hat{\sigma}}I_1(\hat{k}\hat{R}), \tag{5.23}$$

$$\hat{F}_2 = 2\imath\hat{k}\hat{k}_\ell\left(\frac{\mathrm{d}I_1(\hat{k}_\ell\hat{R})}{\mathrm{d}(\hat{k}_\ell\hat{R})}\right) - \left(\frac{1}{\hat{R}^2} - \hat{k}^2\right)\imath\frac{\hat{k}}{\hat{\sigma}}I_1(\hat{k}_\ell\hat{R}), \tag{5.24}$$

$$\hat{F}_3 = -R_e\ell\imath\hat{\sigma}K_0(\hat{k}\hat{R}) + 2\imath m\hat{k}^2\left(\frac{\mathrm{d}K_1(\hat{k}\hat{R})}{\mathrm{d}(\hat{k}\hat{R})}\right), \quad \hat{F}_4 = 2\imath m\hat{k}\hat{k}_a\left(\frac{\mathrm{d}K_1(\hat{k}_a\hat{R})}{\mathrm{d}(\hat{k}_a\hat{R})}\right), \tag{5.25}$$

with

$$\hat{k}_\ell = \sqrt{\hat{k}^2 + R_e\hat{\sigma}}, \quad \hat{k}_a = \sqrt{\hat{k}^2 + \frac{R_e\ell}{m}\hat{\sigma}}. \tag{5.26}$$

5.1 Arrangement

The solutions in dimensionless form are given by

$$\hat{\psi}_\ell = \left[\hat{a}_1\hat{r}\frac{I_1(\hat{k}\hat{r})}{I_1(\hat{k}\hat{R})} + \hat{a}_2\hat{r}\frac{I_1(\hat{k}_\ell\hat{r})}{I_1(\hat{k}_\ell\hat{R})}\right]\exp(\hat{\sigma}\hat{t} + \imath\hat{k}\hat{z}) + c.c., \tag{5.27}$$

$$\hat{\psi}_a = \left[\hat{b}_1\hat{r}\frac{K_1(\hat{k}\hat{r})}{K_1(\hat{k}\hat{R})} + \hat{b}_2\hat{r}\frac{K_1(\hat{k}_a\hat{r})}{K_1(\hat{k}_a\hat{R})}\right]\exp(\hat{\sigma}\hat{t} + \imath\hat{k}\hat{z}) + c.c., \tag{5.28}$$

$$\hat{\eta} = \hat{H}\exp(\hat{\sigma}\hat{t} + \imath\hat{k}\hat{z}) + c.c., \tag{5.29}$$

for which the solvability condition is given as the dispersion relation:

$$\begin{vmatrix} 1 & 1 & 1 & 1 \\ \hat{k}\hat{\alpha}_\ell & \hat{k}_\ell\hat{\alpha}_{\ell 2} & -\hat{k}\hat{\alpha}_a & -\hat{k}_a\hat{\alpha}_{a2} \\ 2\hat{k}^2 & \left(\hat{k}^2+\hat{k}_\ell^2\right) & 2m\hat{k}^2 & m\left(\hat{k}^2+\hat{k}_a^2\right) \\ \imath\hat{f}_1 & \imath\hat{f}_2 & -\imath\hat{f}_3 & -\imath\hat{f}_4 \end{vmatrix} = 0, \tag{5.30}$$

where

$$\hat{f}_1 = R_e\hat{\sigma}\hat{\alpha}_\ell + 2\hat{k}^2\hat{\beta}_\ell - \left(\frac{1}{\hat{R}^2} - \hat{k}^2\right)\frac{\hat{k}}{2\hat{\sigma}}, \quad \hat{f}_2 = 2\hat{k}\hat{k}_\ell\hat{\beta}_{\ell 2} - \left(\frac{1}{\hat{R}^2} - \hat{k}^2\right)\frac{\hat{k}}{2\hat{\sigma}}, \tag{5.31}$$

$$\hat{f}_3 = R_e\ell\hat{\sigma}\hat{\alpha}_a + 2m\hat{k}^2\hat{\beta}_a - \left(\frac{1}{\hat{R}^2} - \hat{k}^2\right)\frac{\hat{k}}{2\hat{\sigma}}, \quad \hat{f}_4 = 2m\hat{k}\hat{k}_a\hat{\beta}_{a2} - \left(\frac{1}{\hat{R}^2} - \hat{k}^2\right)\frac{\hat{k}}{2\hat{\sigma}}, \tag{5.32}$$

with

$$\hat{\alpha}_\ell = \frac{I_0(\hat{k}\hat{R})}{I_1(\hat{k}\hat{R})}, \quad \hat{\alpha}_{\ell 2} = \frac{I_0(\hat{k}_\ell\hat{R})}{I_1(\hat{k}_\ell\hat{R})}, \quad \hat{\alpha}_a = \frac{K_0(\hat{k}\hat{R})}{K_1(\hat{k}\hat{R})}, \quad \hat{\alpha}_{a2} = \frac{K_0(\hat{k}_a\hat{R})}{K_1(\hat{k}_a\hat{R})}, \tag{5.33}$$

$$\hat{\beta}_\ell = \hat{\alpha}_\ell - \frac{1}{\hat{k}\hat{R}}, \quad \hat{\beta}_{\ell 2} = \hat{\alpha}_{\ell 2} - \frac{1}{\hat{k}_\ell\hat{R}}, \quad \hat{\beta}_a = \hat{\alpha}_a + \frac{1}{\hat{k}\hat{R}}, \quad \hat{\beta}_{a2} = \hat{\alpha}_{a2} + \frac{1}{\hat{k}_a\hat{R}}, \tag{5.34}$$

$$\hat{k}_\ell = \sqrt{\hat{k}^2 + R_e\hat{\sigma}}, \quad \hat{k}_a = \sqrt{\hat{k}^2 + \frac{R_e\ell}{m}\hat{\sigma}}, \tag{5.35}$$

$$\frac{\partial\hat{\eta}}{\partial\hat{t}} = \hat{u}_\ell = \frac{1}{\hat{r}}\frac{\partial\hat{\psi}_\ell}{\partial\hat{z}} = \hat{u}_a = \frac{1}{\hat{r}}\frac{\partial\hat{\psi}_a}{\partial\hat{z}} \to \hat{a}_1 + \hat{a}_2 + \hat{b}_1 + \hat{b}_2 = 2\imath\frac{\hat{\sigma}}{\hat{k}}\hat{H}. \tag{5.36}$$

Further rearrangement of the determinant in (5.30) is convenient for calculations.

$$\begin{vmatrix} 1 & 1 & -1 & -1 \\ \hat{k}\hat{\alpha}_\ell & \hat{k}_\ell\hat{\alpha}_{\ell 2} & \hat{k}\hat{\alpha}_a & \hat{k}_a\hat{\alpha}_{a2} \\ 2\hat{k}^2 & \left(\hat{k}^2+\hat{k}_\ell^2\right) & -2m\hat{k}^2 & -m\left(\hat{k}^2+\hat{k}_a^2\right) \\ \hat{f}_1 & \hat{f}_2 & \hat{f}_3 & \hat{f}_4 \end{vmatrix} = \begin{vmatrix} 1 & 0 & -1 & 0 \\ \hat{k}\hat{\alpha}_\ell & \hat{k}_\ell\hat{\alpha}_{\ell 2} - \hat{k}\hat{\alpha}_\ell & \hat{k}\hat{\alpha}_a & \hat{k}_a\hat{\alpha}_{a2} - \hat{k}\hat{\alpha}_a \\ 2\hat{k}^2 & \hat{k}_\ell^2 - \hat{k}^2 & -2m\hat{k}^2 & -m\left(\hat{k}_a^2 - \hat{k}^2\right) \\ \hat{f}_1 & \hat{f}_2 - \hat{f}_1 & \hat{f}_3 & \hat{f}_4 - \hat{f}_3 \end{vmatrix}$$

$$= \begin{vmatrix} 1 & 0 & 0 & 0 \\ \hat{k}\hat{\alpha}_\ell & \hat{k}_\ell\hat{\alpha}_{\ell 2} - \hat{k}\hat{\alpha}_\ell & \hat{k}\left(\hat{\alpha}_a + \hat{\alpha}_\ell\right) & \hat{k}_a\hat{\alpha}_{a2} - \hat{k}\hat{\alpha}_a \\ 2\hat{k}^2 & \hat{k}_\ell^2 - \hat{k}^2 & 2\left(1-m\right)\hat{k}^2 & -m\left(\hat{k}_a^2 - \hat{k}^2\right) \\ \hat{f}_1 & \hat{f}_2 - \hat{f}_1 & \hat{f}_3 + \hat{f}_1 & \hat{f}_4 - \hat{f}_3 \end{vmatrix} = 0 \tag{5.37}$$

In deriving this determinant, the second column has been assigned to $\hat{a}_2$, and the fourth column has been assigned to $\hat{b}_2$. The second row has been assigned to the continuity of tangential velocity, and the third row has been assigned to the tangential stress balance. If these are taken out from the above, the resultant determinant gives $\hat{f}_1 + \hat{f}_3 = 0$, which is the dispersion relation in [VPF].

Then the determinant is expanded as

$$\begin{vmatrix} \hat{k}_\ell\hat{\alpha}_{\ell 2} - \hat{k}\hat{\alpha}_\ell & \hat{k}\left(\hat{\alpha}_a + \hat{\alpha}_\ell\right) & \hat{k}_a\hat{\alpha}_{a2} - \hat{k}\hat{\alpha}_a \\ \hat{k}_\ell^2 - \hat{k}^2 & 2\left(1-m\right)\hat{k}^2 & -m\left(\hat{k}_a^2 - \hat{k}^2\right) \\ \hat{f}_2 - \hat{f}_1 & \hat{f}_3 + \hat{f}_1 & \hat{f}_4 - \hat{f}_3 \end{vmatrix} = \left(\hat{f}_2 - \hat{f}_1\right) \begin{vmatrix} \hat{k}\left(\hat{\alpha}_a + \hat{\alpha}_\ell\right) & \hat{k}_a\hat{\alpha}_{a2} - \hat{k}\hat{\alpha}_a \\ 2\left(1-m\right)\hat{k}^2 & -m\left(\hat{k}_a^2 - \hat{k}^2\right) \end{vmatrix} \tag{5.38}$$

$$- \left(\hat{f}_3 + \hat{f}_1\right) \begin{vmatrix} \hat{k}_\ell\hat{\alpha}_{\ell 2} - \hat{k}\hat{\alpha}_\ell & \hat{k}_a\hat{\alpha}_{a2} - \hat{k}\hat{\alpha}_a \\ \hat{k}_\ell^2 - \hat{k}^2 & -m\left(\hat{k}_a^2 - \hat{k}^2\right) \end{vmatrix} + \left(\hat{f}_4 - \hat{f}_3\right) \begin{vmatrix} \hat{k}_\ell\hat{\alpha}_{\ell 2} - \hat{k}\hat{\alpha}_\ell & \hat{k}\left(\hat{\alpha}_a + \hat{\alpha}_\ell\right) \\ \hat{k}_\ell^2 - \hat{k}^2 & 2\left(1-m\right)\hat{k}^2 \end{vmatrix} = 0. \tag{5.39}$$

If $\hat{k}_\ell$ and $\hat{k}_a$ are approximated as

$$\hat{k}_\ell = \sqrt{\hat{k}^2 + R_e\hat{\sigma}} \approx k + \frac{R_e\hat{\sigma}}{2k}, \quad \hat{k}_a = \sqrt{\hat{k}^2 + \frac{R_e\ell}{m}\hat{\sigma}} \approx k + \frac{R_e\ell}{2km}\hat{\sigma}. \tag{5.40}$$

we have

$$\hat{f}_2 - \hat{f}_1 = 2\hat{k}\hat{k}_\ell\hat{\beta}_{\ell 2} - R_e\hat{\sigma}\hat{\alpha}_\ell - 2\hat{k}^2\hat{\beta}_\ell = 2\hat{k}\left(\hat{k}_\ell\hat{\beta}_{\ell 2} - \hat{k}\hat{\beta}_\ell\right) - R_e\hat{\sigma}\hat{\alpha}_\ell \tag{5.41}$$

$$\hat{f}_4 - \hat{f}_3 = 2m\hat{k}\hat{k}_a\hat{\beta}_{a2} - R_e\ell\hat{\sigma}\hat{\alpha}_a - 2m\hat{k}^2\hat{\beta}_a = 2m\hat{k}\left(\hat{k}_a\hat{\beta}_{a2} - \hat{k}\hat{\beta}_a\right) - R_e\ell\hat{\sigma}\hat{\alpha}_a \tag{5.42}$$

6 Linear theory of stability for VPF

The equations given in section 4 are linearized and solutions of the linearized equations are taken in the following form:

$$\psi_\ell = A_1 r I_1(kr)\exp(\sigma t + \imath kz) + c.c., \tag{6.1}$$

$$\psi_a = B_1 r K_1(kr)\exp(\sigma t + \imath kz) + c.c., \tag{6.2}$$

$$\eta = H\exp(\sigma t + \imath kz) + c.c. \tag{6.3}$$

The kinematic condition is given by

$$\imath k A_1 I_1(kR) = \sigma H, \quad \imath k B_1 K_1(kR) = \sigma H. \tag{6.4}$$

The normal stress balance is expressed as

$$\imath\sigma\rho_\ell A_1 I_0(kR) + 2\mu_\ell \imath k^2 A_1 \left(\frac{\mathrm{d}I_1(kR)}{\mathrm{d}(kR)}\right) + \imath\sigma\rho_a B_1 K_0(kR) - 2\mu_a \imath k^2 B_1 \left(\frac{\mathrm{d}K_1(kR)}{\mathrm{d}(kR)}\right) = \gamma\left(\frac{1}{R^2} - k^2\right) H, \tag{6.5}$$

thus we have

$$\begin{aligned} &\rho_\ell\sigma^2 \frac{I_0(kR)}{I_1(kR)} H + 2\mu_\ell k^2 \frac{\sigma}{I_1(kR)}\left(I_0(kR) - \frac{I_1(kR)}{kR}\right) H \\ &+\rho_a\sigma^2 \frac{K_0(kR)}{K_1(kR)} H - 2\mu_a k^2 \frac{\sigma}{K_1(kR)}\left(-K_0(kR) - \frac{K_1(kR)}{kR}\right) H = \gamma\left(\frac{1}{R^2} - k^2\right) kH, \end{aligned} \tag{6.6}$$

then the dispersion relation is given by

$$\rho_\ell\sigma^2\alpha_\ell(kR) + 2\mu_\ell k^2\sigma\beta_\ell(kR) + \rho_a\sigma^2\alpha_a(kR) + 2\mu_a k^2\sigma\beta_a(kR) = \gamma\left(\frac{1}{R^2} - k^2\right) k, \tag{6.7}$$

with

$$\alpha_\ell(kR) = \frac{I_0(kR)}{I_1(kR)}, \quad \alpha_a(kR) = \frac{K_0(kR)}{K_1(kR)}, \quad \beta_\ell(kR) = \alpha_\ell(kR) - \frac{1}{kR}, \quad \beta_a(kR) = \alpha_a(kR) + \frac{1}{kR}.$$

The analysis in terms of the stream function coincides with that made before in terms of the potential.

The solutions in dimensionless form are given by

$$\hat{\psi}_\ell = \hat{A}_1 \hat{r} I_1(\hat{k}\hat{r}) \exp(\hat{\sigma}\hat{t} + \imath\hat{k}\hat{z}) + c.c.,$$

$$\hat{\psi}_a = \hat{B}_1 \hat{r} K_1(\hat{k}\hat{r}) \exp(\hat{\sigma}\hat{t} + \imath\hat{k}\hat{z}) + c.c.,$$

$$\hat{\eta} = \hat{H} \exp(\hat{\sigma}\hat{t} + \imath\hat{k}\hat{z}) + c.c.$$

The dispersion relation is given in dimensionless form

$$\left(\hat{\alpha}_\ell + \ell\hat{\alpha}_a\right)\hat{\sigma}^2 + 2\hat{k}^2\left(\hat{\mu}_\ell\hat{\beta}_\ell + \hat{\mu}_a\hat{\beta}_a\right)\hat{\sigma} = \left(\frac{1}{\hat{R}^2} - \hat{k}^2\right)\hat{k}, \tag{6.8}$$

with

$$\hat{\alpha}_\ell = \frac{I_0(\hat{k}\hat{R})}{I_1(\hat{k}\hat{R})}, \quad \hat{\alpha}_a = \frac{K_0(\hat{k}\hat{R})}{K_1(\hat{k}\hat{R})}, \quad \hat{\beta}_\ell = \hat{\alpha}_\ell - \frac{1}{\hat{k}\hat{R}}, \quad \hat{\beta}_a = \hat{\alpha}_a + \frac{1}{\hat{k}\hat{R}}, \tag{6.9}$$

$$\hat{\sigma} = -\frac{\hat{k}^2\left(\hat{\mu}_\ell\hat{\beta}_\ell + \hat{\mu}_a\hat{\beta}_a\right)}{\left(\hat{\alpha}_\ell + \ell\hat{\alpha}_a\right)} \pm \sqrt{\left[\frac{\hat{k}^2\left(\hat{\mu}_\ell\hat{\beta}_\ell + \hat{\mu}_a\hat{\beta}_a\right)}{\left(\hat{\alpha}_\ell + \ell\hat{\alpha}_a\right)}\right]^2 + \frac{\left(\frac{1}{\hat{R}^2} - \hat{k}^2\right)\hat{k}}{\left(\hat{\alpha}_\ell + \ell\hat{\alpha}_a\right)}} \tag{6.10}$$

No.	material (fluid ℓ - fluid a)
1	mercury-air
2	mercury-water
3	water-air
4	benzene-air
5	water-benzene
6	SO100-air
7	glycerine-mercury
8	glycerine-air
9	oil-air
10	goldensyrup-CC4 and paraffin
11	SO10000-air
12	goldensyrup-BBoil
13	goldensyrup-Black lubrication oil
14	tar pitch mixture-goldensyrup

Table 7.1: *Fluid pairs for study of capillary instability when the viscous fluid is inside. An additional 14 pairs numbered from 15-28 are obtained by inverting 1-14 so that the viscous fluid is outside; for example, 15 is air-mercury. These 28 fluid pairs are the data base for this paper.*

No.	ρ_ℓ (g/cc)	μ_ℓ (P)	ρ_a (g/cc)	μ_a (P)	γ (dyn/cm))
1	1.3500E+01	1.5600E-02	1.2000E-03	1.8000E-04	4.8210E+02
2	1.3500E+01	1.5600E-02	1.0000E+00	1.0000E-02	3.7500E+02
3	1.0000E+00	1.0000E-02	1.2000E-03	1.8000E-04	7.2800E+01
4	8.6000E-01	6.5000E-03	1.2000E-03	1.8000E-04	2.8860E+01
5	1.0000E+00	1.0000E-02	8.6000E-01	6.5000E-03	3.2800E+01
6	9.6900E-01	1.0000E+00	1.2000E-03	1.8000E-04	2.1000E+01
7	1.2570E+00	7.8200E+00	1.3500E+01	1.5600E-02	3.7500E+02
8	1.2570E+00	7.8200E+00	1.2000E-03	1.8000E-04	6.3400E+01
9	8.7980E-01	4.8300E+00	1.3000E-03	1.8500E-04	3.1500E+01
10	1.4000E+00	1.1000E+02	1.6000E+00	3.4000E-02	2.3000E+01
11	9.6900E-01	1.0000E+02	1.2000E-03	1.8000E-04	2.1000E+01
12	1.4000E+00	1.1000E+02	9.0000E-01	6.0000E+01	1.7000E+01
13	1.4000E+00	1.1000E+02	8.5000E-01	1.0000E+02	8.0000E+00
14	1.4000E+00	2.0000E+03	1.4000E+00	1.1000E+02	2.3000E+01

Table 7.2: *Density (g/cc), viscosity (P) and interfacial tension (dyn/cm) for fluids in table 7.1.*

No.	ℓ	m	No.	ℓ	m	J
1	8.889E-05	1.154E-02	15	1.125E+04	8.667E+01	2.674E+07
2	7.407E-02	6.410E-01	16	1.350E+01	1.560E+00	2.080E+07
3	1.200E-03	1.800E-02	17	8.333E+02	5.556E+01	7.280E+05
4	1.395E-03	2.769E-02	18	7.167E+02	3.611E+01	5.874E+05
5	8.600E-01	6.500E-01	19	1.163E+00	1.538E+00	3.280E+05
6	1.238E-03	1.800E-04	20	8.075E+02	5.556E+03	2.035E+01
7	1.074E+01	1.995E-03	21	9.311E-02	5.013E+02	7.708E+00
8	9.547E-04	2.302E-05	22	1.048E+03	4.344E+04	1.303E+00
9	1.478E-03	3.830E-05	23	6.768E+02	2.611E+04	1.188E+00
10	1.143E+00	3.091E-04	24	8.750E-01	3.235E+03	2.661E-03
11	1.238E-03	1.800E-06	25	8.075E+02	5.556E+05	2.035E-03
12	6.429E-01	5.455E-01	26	1.556E+00	1.833E+00	1.967E-03
13	6.071E-01	9.091E-01	27	1.647E+00	1.100E+00	9.256E-04
14	1.000E+00	5.500E-02	28	1.000E+00	1.818E+01	8.050E-06

Table 7.3: *Dimensionless parameters $\ell = \rho_a/\rho_\ell, m = \mu_a/\mu_\ell$ and $J = \rho\gamma D/\mu^2$ is a Reynolds number based on the maximum viscosity, which is the viscosity μ_ℓ listed in table 7.2. Entries 15-28 are for cases in which μ_ℓ and ρ_ℓ are for the outside fluid.*

7 Analysis of dimensionless growth rate curves, σ(sec^{-1}) vs. k(cm^{-1})

Growth rate curves were computed for 14 fluid pairs; ℓ, a are listed in table 7.1.

The density, viscosity and interfacial tension of the fluids in table 7.1 are listed in table 7.2.

In table 7.3 we list the 28 values of dimensionless parameters needed to calculate growth rates for fully viscous flow; 14 when the more viscous liquid is inside and an additional 14 when the more viscous liquid is outside.

Growth rate curves σ(sec^{-1}) vs. k(cm^{-1}) for the 14 fluids listed in table 7.1 are given in figures 7.1–7.14. The computation was carried out with $D = 1$ cm. The inverse case, with the viscous fluid outside, is plotted in figures 7.15 to 7.28. There are three curves in each figure belonging to fully viscous, viscous potential and inviscid potential flow. The curves have a universal order with the highest growth given by inviscid potential flow (IPF) and the lowest growth rates by fully viscous flow.

Table 7.4 lists the maximum growth rate and the wavenumber of maximum growth for fully viscous and viscous potential flow. We measure the agreement by monitoring the ratio of maximum growth rates σ_{MV}/σ_{MF} and the ratio of the maximizing wavenumbers. The agreement is good when these ratios are nearly one. Table 7.4 shows very good agreements for high Reynolds numbers greater than O(10^4) and reasonable agreement for Reynolds numbers greater than O(1).

We call the readers attention to the fact that the agreements between fully viscous and viscous potential flow are good when J is large, even the fluid when the pairs are two liquids. This result is in apparent disagreement with the notion that such agreements are somehow associated with the behavior of boundary layers at gas-liquid surfaces (see section 9.)

No.	J	k_{mV}	σ_{mV}	k_{mF}	σ_{mF}	k_{mV}/k_{mF}	σ_{mV}/σ_{mF}
1	2.6744E+07	1.3957E+00	1.8774E-04	1.3957E+00	1.8766E-04	1.0000E+00	1.0004E+00
2	2.0803E+07	1.3894E+00	2.1122E-04	1.3894E+00	2.0942E-04	1.0000E+00	1.0086E+00
3	2.0803E+07	1.2814E+00	1.8446E-04	1.2929E+00	1.8120E-04	9.9105E-01	1.0180E+00
4	7.2800E+05	1.3957E+00	1.1366E-03	1.3894E+00	1.1334E-03	1.0045E+00	1.0028E+00
5	5.8745E+05	1.3957E+00	1.2650E-03	1.3894E+00	1.2609E-03	1.0045E+00	1.0033E+00
6	3.2800E+05	1.3585E+00	1.5597E-03	1.3524E+00	1.4827E-03	1.0045E+00	1.0519E+00
7	3.1834E+04	2.4931E-01	2.8156E-04	4.0520E-01	2.6573E-04	6.1527E-01	1.0596E+00
8	2.0349E+01	1.2416E+00	1.7491E-01	1.0898E+00	1.3151E-01	1.1393E+00	1.3299E+00
9	1.3032E+00	9.8716E-01	4.5010E-01	7.4027E-01	2.4080E-01	1.3335E+00	1.8692E+00
10	1.1880E+00	9.7832E-01	4.6134E-01	7.3035E-01	2.4384E-01	1.3395E+00	1.8920E+00
11	4.2500E-03	1.6858E-01	3.3993E-01	1.1870E+00	5.1117E-02	1.4202E-01	6.6500E+00
12	2.0349E-03	2.7772E-01	9.5215E-01	1.7397E-01	3.2835E-01	1.5963E+00	2.8998E+00
13	6.8000E-04	1.2585E-01	4.6677E-01	1.1298E+00	6.7419E-02	1.1140E-01	6.9235E+00
14	8.0500E-06	6.7356E-02	9.4484E-01	7.2381E-01	2.2728E-01	9.3057E-02	4.1572E+00
15	2.6744E+07	9.6956E-01	5.1715E-06	9.6956E-01	5.1697E-06	1.0000E+00	1.0003E+00
16	2.0803E+07	1.1659E+00	2.6645E-04	1.1764E+00	2.6015E-04	9.9105E-01	1.0242E+00
17	2.0803E+07	1.0704E+00	1.7136E-01	9.9608E-01	1.2297E-01	1.0746E+00	1.3935E+00
18	7.2800E+05	9.7394E-01	4.8597E-05	9.7394E-01	4.8447E-05	1.0000E+00	1.0031E+00
19	5.8745E+05	9.7394E-01	8.3145E-05	9.7832E-01	8.2776E-05	9.9551E-01	1.0045E+00
20	3.2800E+05	1.3463E+00	1.0658E-03	1.3403E+00	1.0102E-03	1.0045E+00	1.0550E+00
21	3.1834E+04	2.9710E-01	9.4473E-01	2.7523E-01	3.2087E-01	1.0795E+00	2.9442E+00
22	2.0349E+01	6.3246E-01	6.4779E-05	6.2962E-01	6.3660E-05	1.0045E+00	1.0176E+00
23	1.3032E+00	2.9577E-01	1.7161E-05	3.2653E-01	1.7034E-05	9.0580E-01	1.0075E+00
24	1.1880E+00	2.9710E-01	2.8893E-05	3.3849E-01	2.8594E-05	8.7773E-01	1.0105E+00
25	4.2500E-03	2.0181E-01	6.2177E-01	1.1046E+00	9.7961E-02	1.8269E-01	6.3471E+00
26	2.0349E-03	3.9264E-02	1.7918E-06	1.0608E-01	1.7787E-06	3.7013E-01	1.0073E+00
27	6.8000E-04	1.4468E-01	5.1111E-01	1.1196E+00	7.4787E-02	1.2922E-01	6.8342E+00
28	8.0500E-06	5.1426E-02	5.1834E-02	1.0898E+00	1.5879E-02	4.7188E-02	3.2644E+00

Table 7.4: *Maximum growth rate and the associated wavenumber ratios indexed by J; cases 1-14 are viscous fluid inside, 15-28 for viscous fluid outside. The ratios are nearly one, indicating agreement between FVF and VPF when J is large.*

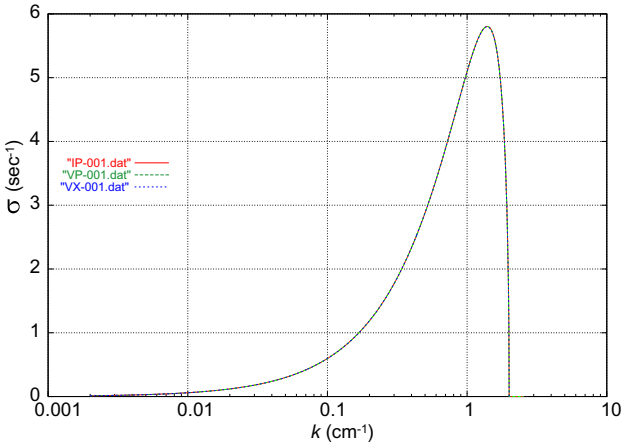

Figure 7.1: *Mercury in air.*

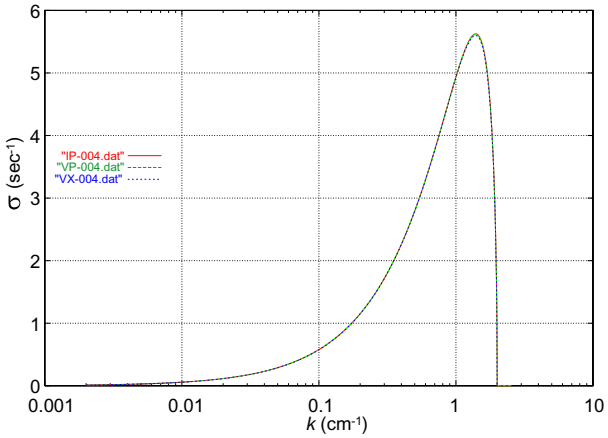

Figure 7.4: *Benzene in air.*

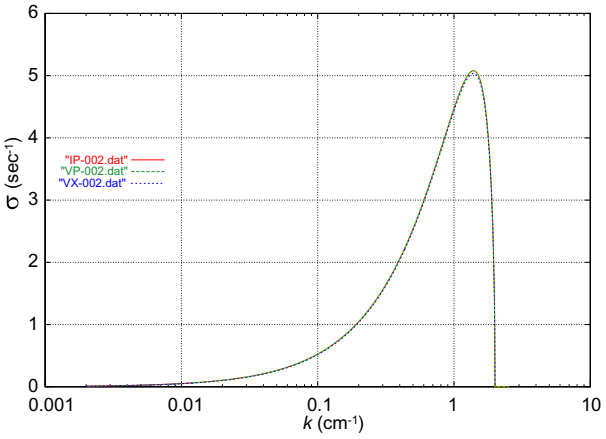

Figure 7.2: *Mercury in water.*

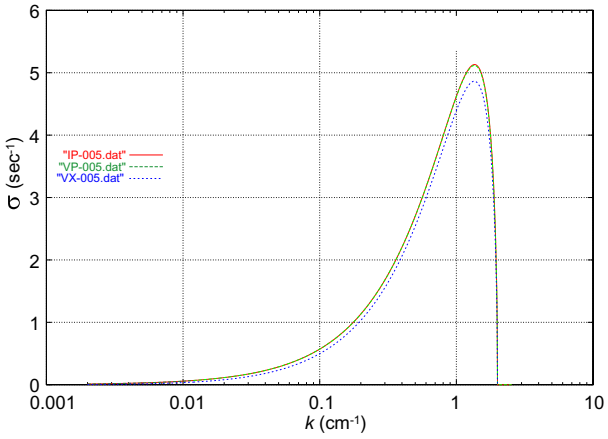

Figure 7.5: *Water in Benzene.*

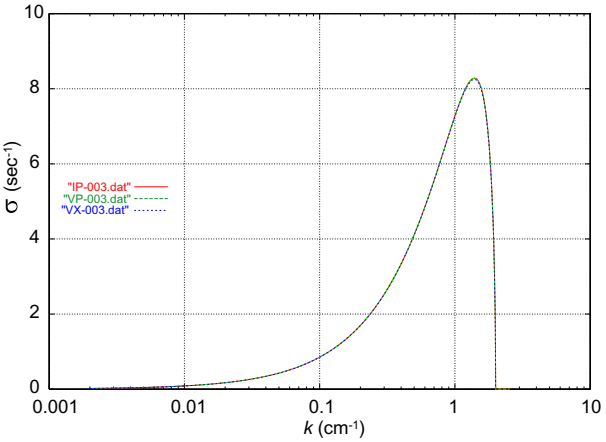

Figure 7.3: *Water in air.*

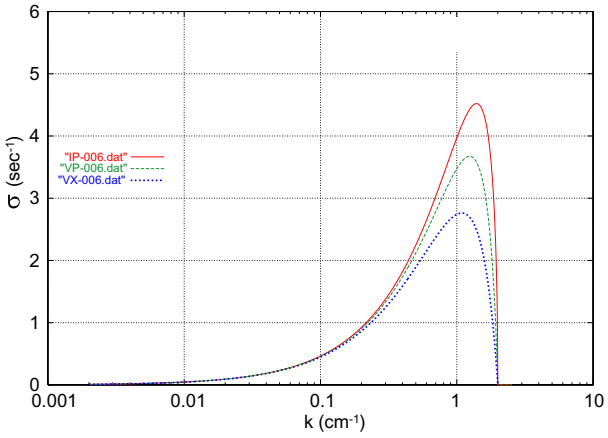

Figure 7.6: *SO100 in air.*

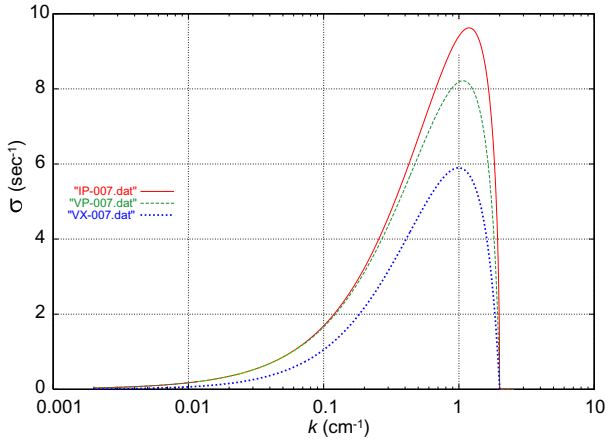

Figure 7.7: *Glycerine in mercury.*

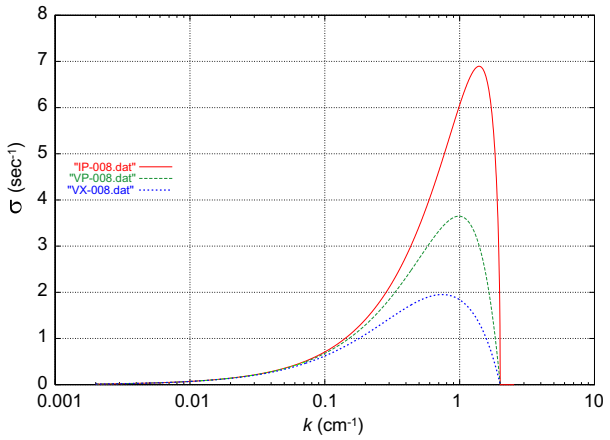

Figure 7.8: *Glycerine in air.*

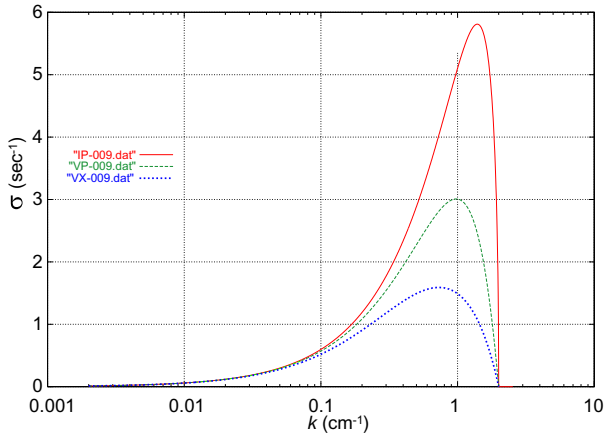

Figure 7.9: *Oil in air.*

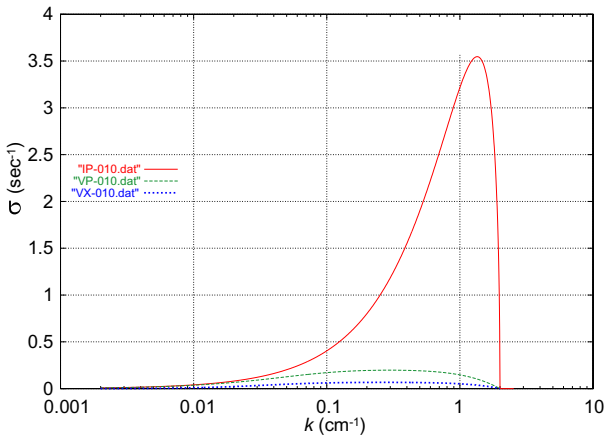

Figure 7.10: *Goldensyrup in paraffin.*

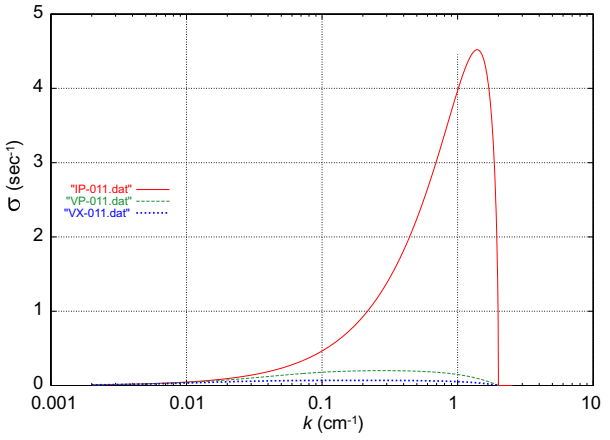

Figure 7.11: *SO10000 in air.*

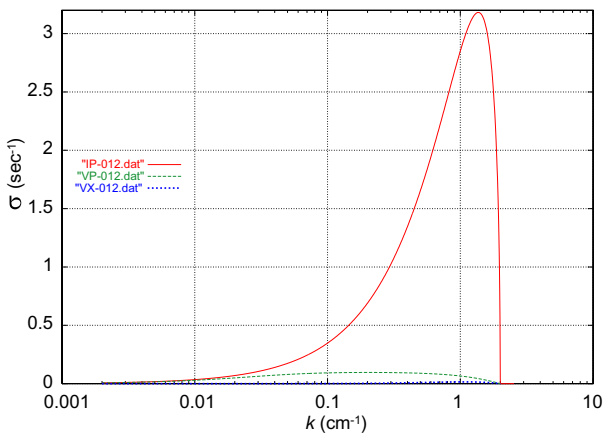

Figure 7.12: *Goldensyrup in BB oil.*

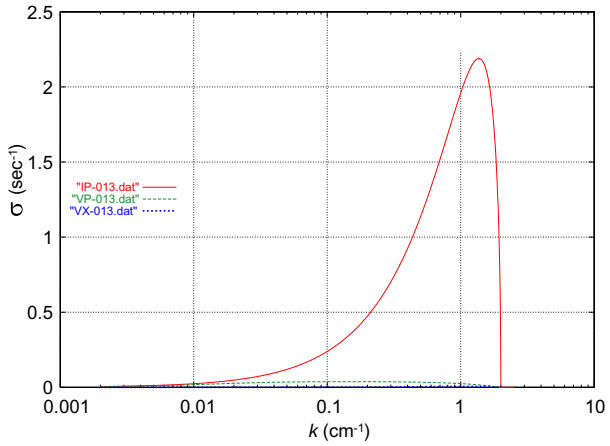

Figure 7.13: *Goldensyrup in black lubrication oil.*

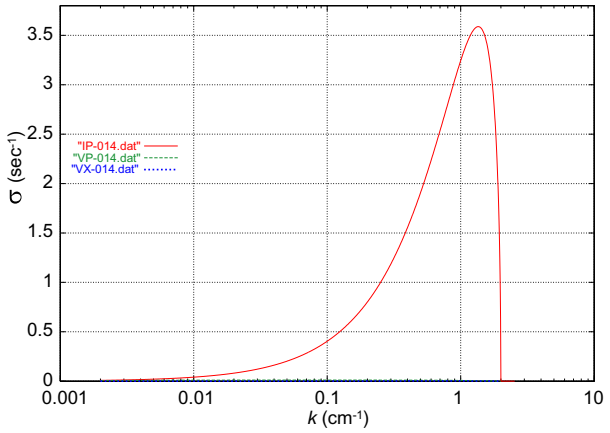

Figure 7.14: *Tar pitch mixture in goldensyrup.*

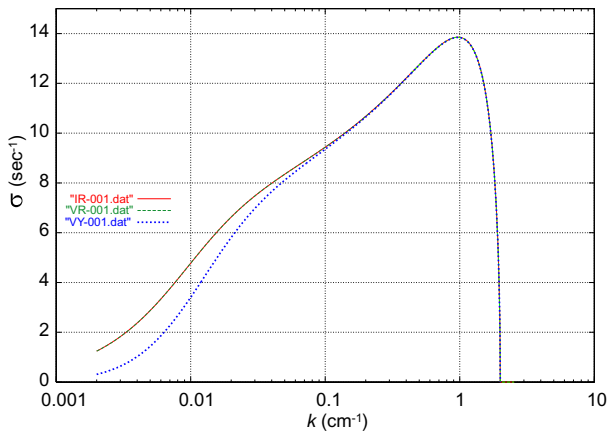

Figure 7.15: *Air in mercury.*

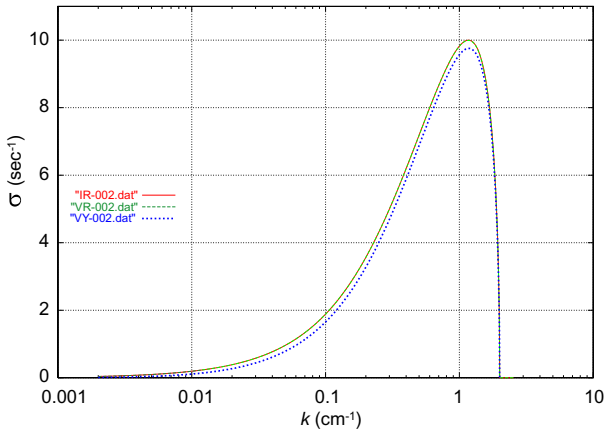

Figure 7.16: *Water in mercury.*

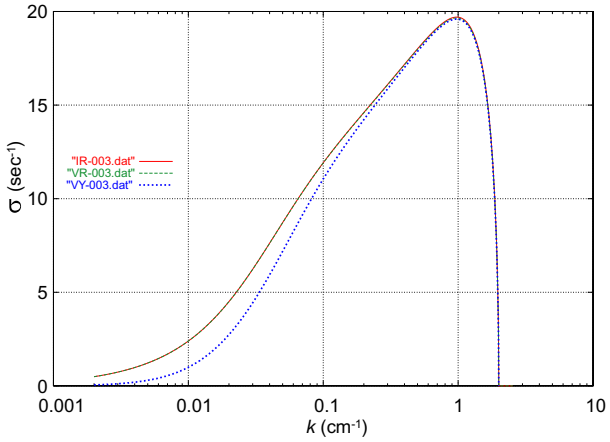

Figure 7.17: *Air in water.*

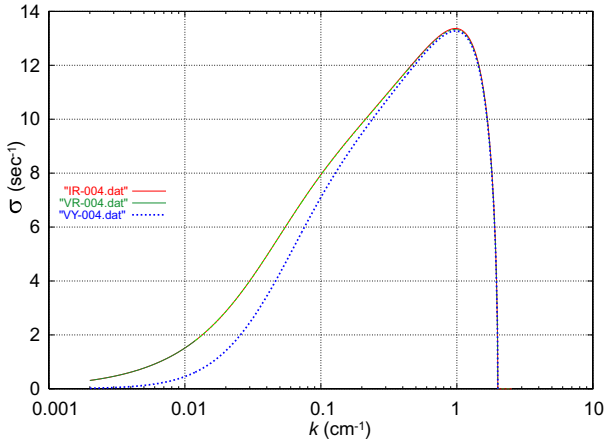

Figure 7.18: *Air in benzene.*

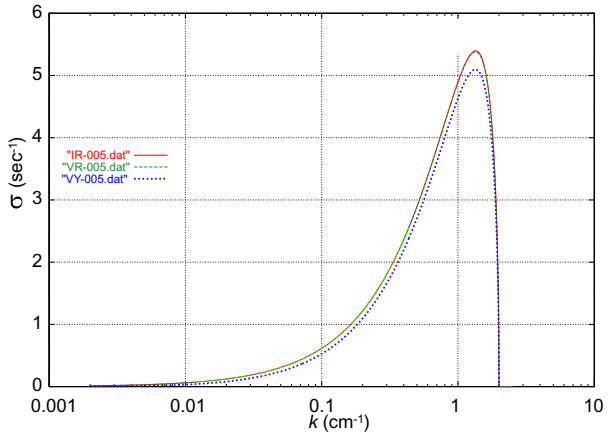

Figure 7.19: *Benzene in water.*

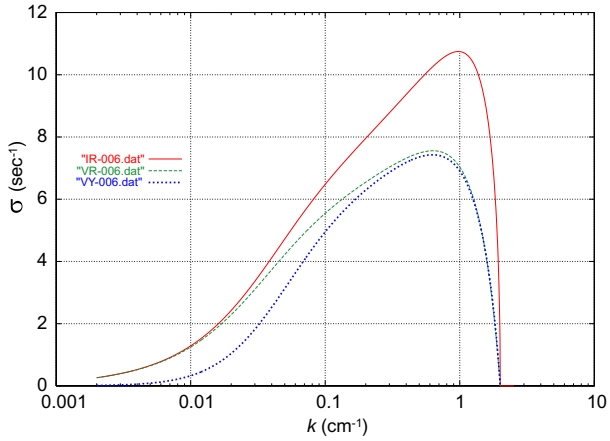

Figure 7.20: *Air in SO100.*

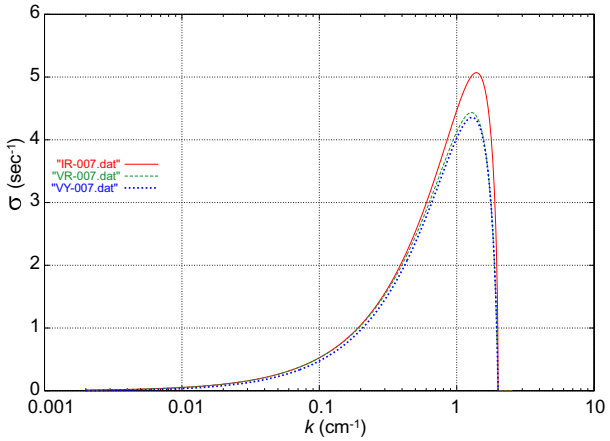

Figure 7.21: *Mercury in glycerine.*

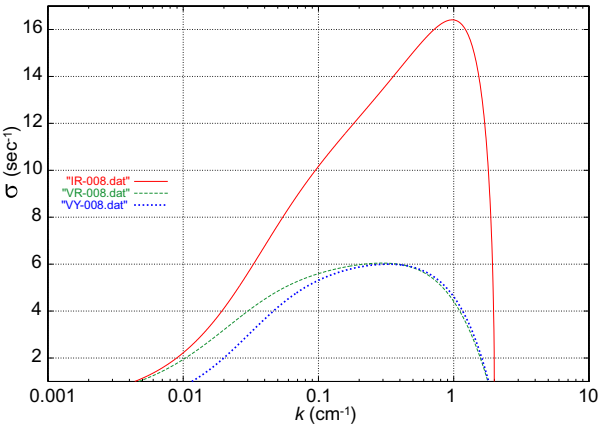

Figure 7.22: *Air in glycerine.*

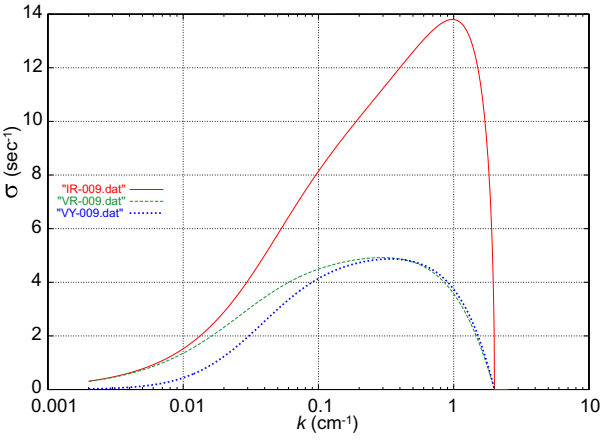

Figure 7.23: *Air in oil.*

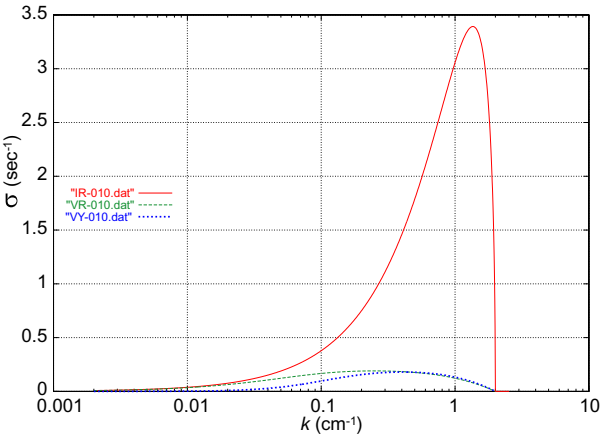

Figure 7.24: *Paraffin in goldensyrup.*

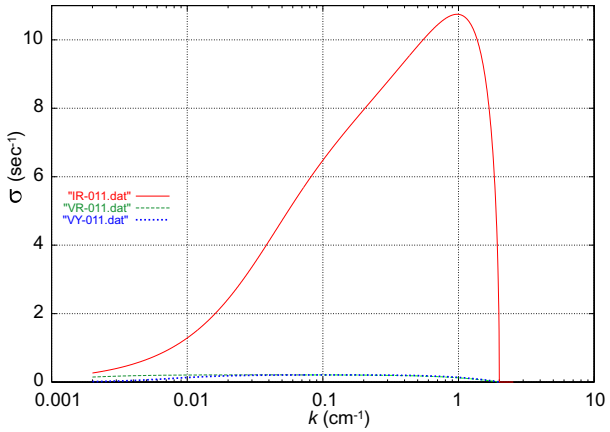

Figure 7.25: *Air in SO10000.*

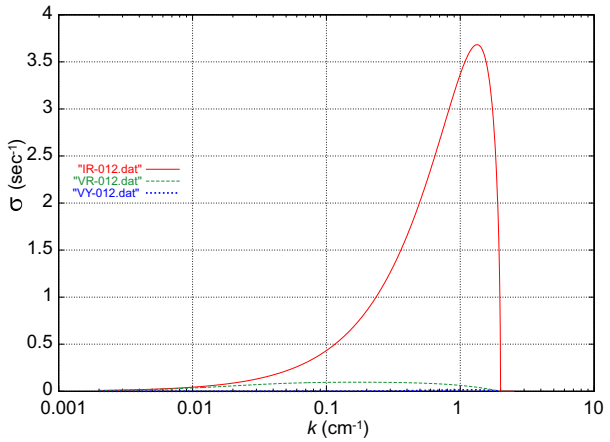

Figure 7.26: *BB oil in goldensyrup.*

In table 7.5 we give the growth rate ratios and associated wavenumber ratios for viscous and inviscid potential flow.

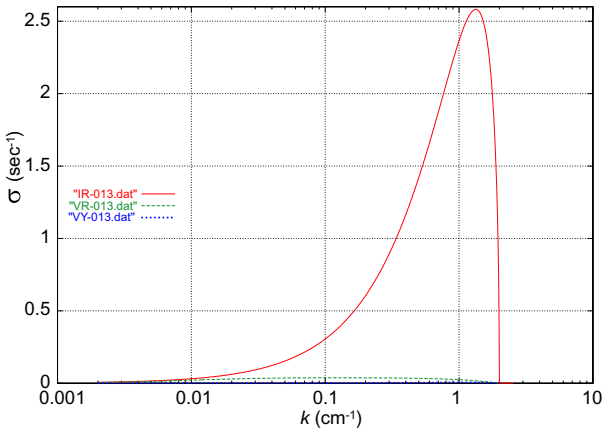

Figure 7.27: *Black lubrication oil in goldensyrup.*

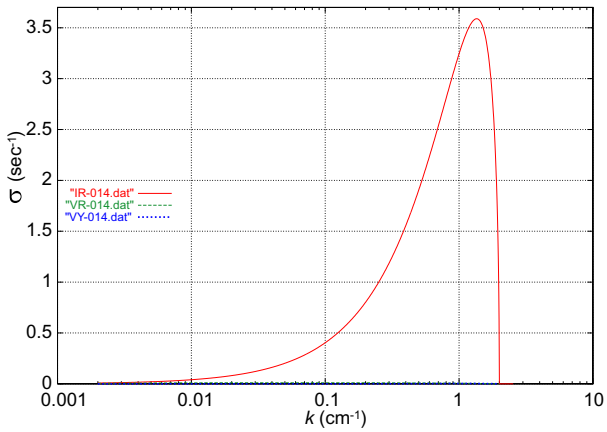

Figure 7.28: *Goldensyrup in tar pitch mixture.*

No.	k_{mI}	σ_{mI}	k_{mV}	σ_{mV}	k_{mV}/k_{mI}	σ_{mV}/σ_{mI}
1	1.3957E+00	5.8032E+00	1.3957E+00	5.8020E+00	1.0000E+00	9.9979E-01
2	1.3894E+00	5.0795E+00	1.3894E+00	5.0774E+00	1.0000E+00	9.9958E-01
3	1.3957E+00	8.2847E+00	1.3957E+00	8.2742E+00	1.0000E+00	9.9873E-01
4	1.3957E+00	5.6247E+00	1.3957E+00	5.6167E+00	1.0000E+00	9.9857E-01
5	1.3585E+00	5.1309E+00	1.3585E+00	5.1158E+00	1.0000E+00	9.9704E-01
6	1.3957E+00	4.5202E+00	1.2416E+00	3.6731E+00	8.8965E-01	8.1258E-01
7	1.1924E+00	9.6266E+00	1.0704E+00	8.2173E+00	8.9769E-01	8.5361E-01
8	1.3957E+00	6.8961E+00	9.8716E-01	3.6491E+00	7.0731E-01	5.2916E-01
9	1.3957E+00	5.8098E+00	9.7832E-01	3.0087E+00	7.0098E-01	5.1786E-01
10	1.3463E+00	3.5469E+00	2.9710E-01	1.9753E-01	2.2067E-01	5.5692E-02
11	1.3957E+00	4.5202E+00	2.7772E-01	1.9995E-01	1.9899E-01	4.4235E-02
12	1.3646E+00	3.1816E+00	2.0181E-01	9.6092E-02	1.4788E-01	3.0202E-02
13	1.3708E+00	2.1896E+00	1.4468E-01	3.7171E-02	1.0554E-01	1.6977E-02
14	1.3524E+00	3.5887E+00	6.7356E-02	1.0866E-02	4.9804E-02	3.0277E-03
15	9.6956E-01	1.3856E+01	9.6956E-01	1.3851E+01	1.0000E+00	9.9963E-01
16	1.1711E+00	9.9984E+00	1.1659E+00	9.9919E+00	9.9551E-01	9.9936E-01
17	9.7394E-01	1.9700E+01	9.7394E-01	1.9655E+01	1.0000E+00	9.9772E-01
18	9.7832E-01	1.3365E+01	9.7394E-01	1.3331E+01	9.9551E-01	9.9744E-01
19	1.3463E+00	5.3956E+00	1.3463E+00	5.3782E+00	1.0000E+00	9.9679E-01
20	9.7394E-01	1.0747E+01	6.3246E-01	7.5576E+00	6.4938E-01	7.0324E-01
21	1.3894E+00	5.0698E+00	1.2814E+00	4.4341E+00	9.2224E-01	8.7462E-01
22	9.7394E-01	1.6413E+01	2.9577E-01	6.0446E+00	3.0368E-01	3.6829E-01
23	9.7832E-01	1.3801E+01	2.9710E-01	4.9196E+00	3.0368E-01	3.5647E-01
24	1.3585E+00	3.3924E+00	2.4931E-01	1.9046E-01	1.8352E-01	5.6144E-02
25	9.7394E-01	1.0747E+01	3.9264E-02	2.0904E-01	4.0315E-02	1.9451E-02
26	1.3343E+00	3.6829E+00	1.6858E-01	9.6312E-02	1.2635E-01	2.6151E-02
27	1.3343E+00	2.5820E+00	1.2585E-01	3.7342E-02	9.4321E-02	1.4462E-02
28	1.3524E+00	3.5887E+00	5.1426E-02	1.0838E-02	3.8026E-02	3.0200E-03

Table 7.5: *Maximum growth rate and wavenumber ratios for VPF and IPF when the viscous liquid is inside (No. 1-14) and outside (No. 15-28).*

8 Analysis of dimensionless growth rate curves $\hat{\sigma}$ vs. $\hat{k}$

The dimensionless growth rate curves $\hat{\sigma}$ vs. $\hat{k}$ depend only on three control parameters ℓ, m and J. The dimensionless description allows for maximum generality. We first show how $\hat{\sigma}_m$ and $\hat{k}_m$ from FVF varies with $\sqrt{J}$ for different values of ℓ and m given in table 8.1.

Name	ℓ	m	Name	ℓ	m
f11	0.01	0.01	f31	100.	0.01
f12	0.01	1.00	f32	100.	1.00
f13	0.01	100.	f33	100.	100.
f14	0.01	1000.	f34	100.	1000.
f21	1.00	0.01	f41	1000.	0.01
f22	1.00	1.00	f42	1000.	1.00
f23	1.00	100.	f43	1000.	100.
f24	1.00	1000.	f44	1000.	1000.

Table 8.1: *Control parameters ℓ and m for the curves $\hat{\sigma}_m$ vs. $\sqrt{J}$ and $\hat{k}_m$ vs. $\sqrt{J}$ in figures 8.1 and 8.2.*

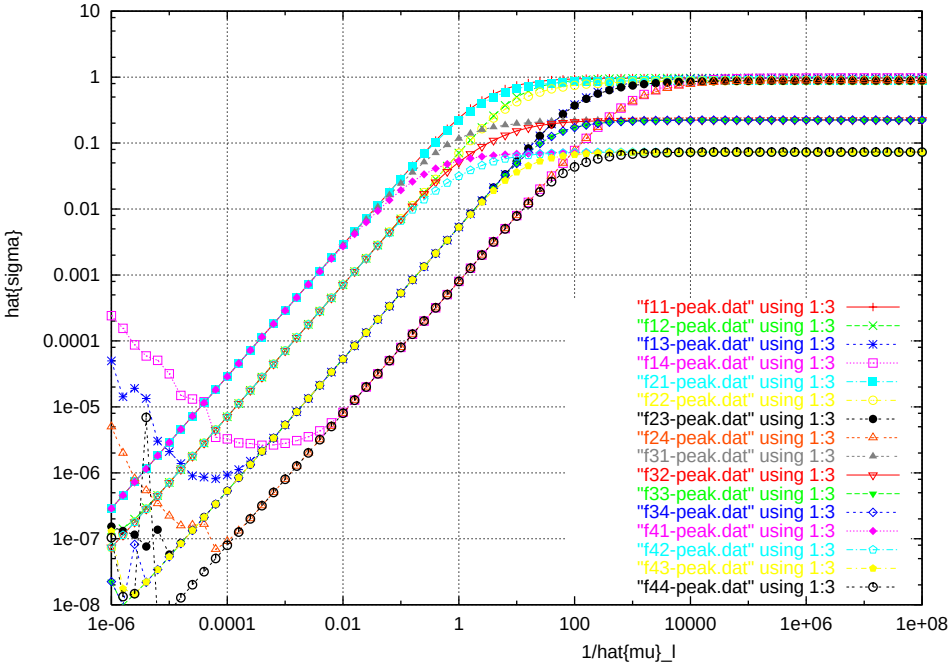

Figure 8.1: *The maximum growth rate $\hat{\sigma}_m$ vs. $\sqrt{J}$ for various values of ℓ and m given in table 8.1. The existence of interior minumum value of $\hat{\sigma}_m$ for small $\sqrt{J}$ and certian values of ℓ and m is noteworthy.*

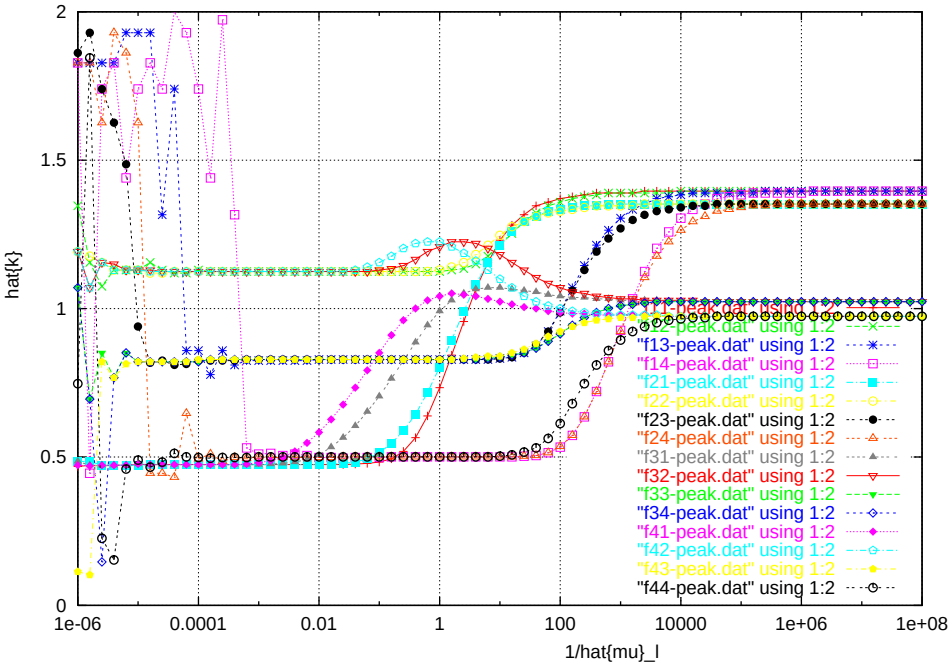

Figure 8.2: *Wavenumber $\hat{k}_m$ vs. $\sqrt{J}$ for the values of ℓ and m in table 8.1. The existence of a maximum value of $\hat{k}_m$ at values of J near 1 for certian values of ℓ and m is noteworthy.*

In figures 8.3–8.30 we plotted the peak values $\hat{\sigma}_m$ and the corresponding wavenumber $\hat{k}_m$ vs. $\sqrt{J}$ for fixed values of ℓ and m which are given in table 7.3. The maximum growth rate $\hat{\sigma}_m$ and $\hat{k}_m$ for IPF do not depend on $\hat{k}_\ell$ and appear as the highest flat value. The smallest growth rate is for FVF.

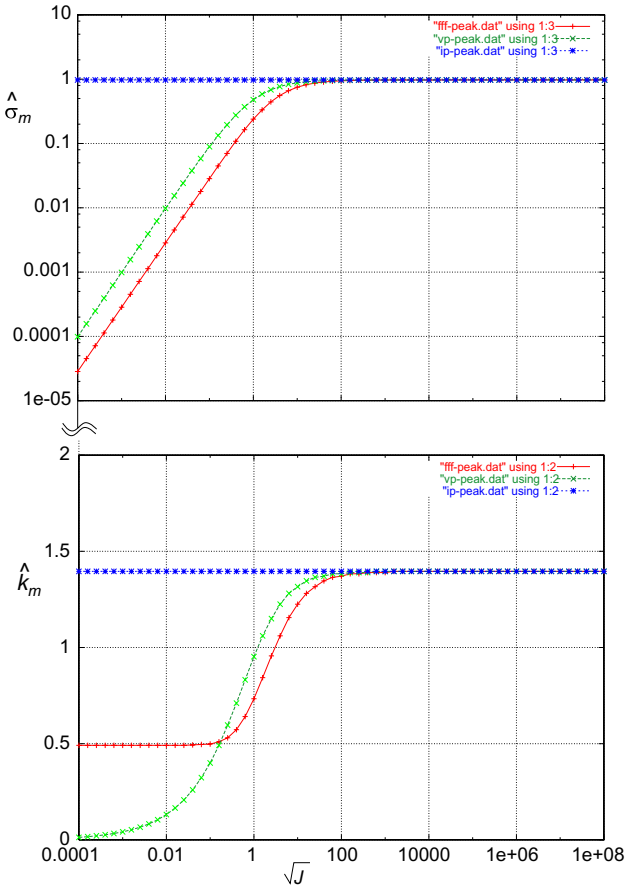

Figure 8.3: *$\hat{\sigma}_m$ and $\hat{k}_m$ vs. $\sqrt{J}$ for values of ℓ and m for mercury and air.*

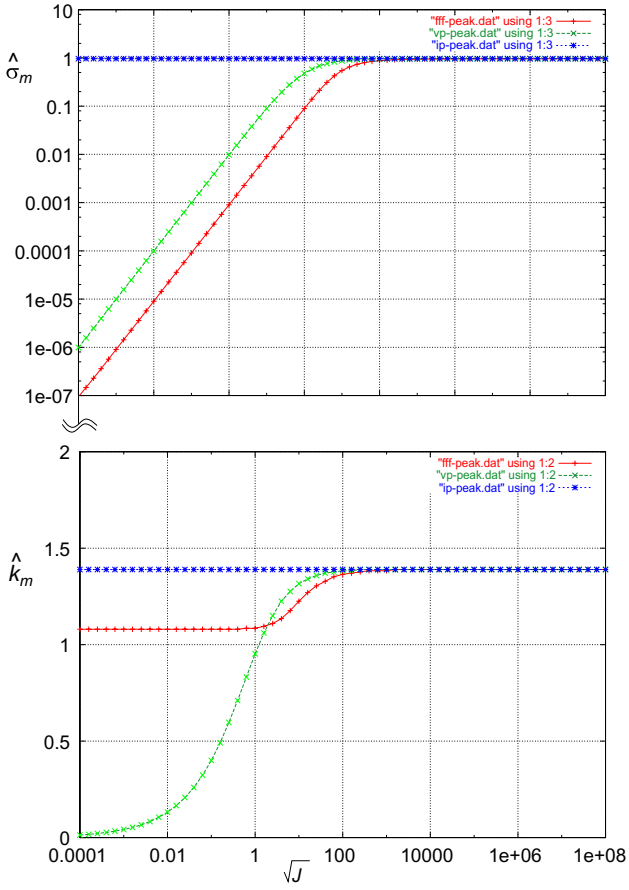

Figure 8.4: *$\hat{\sigma}_m$ and $\hat{k}_m$ vs. $\sqrt{J}$ for values of ℓ and m for mercury and water.*

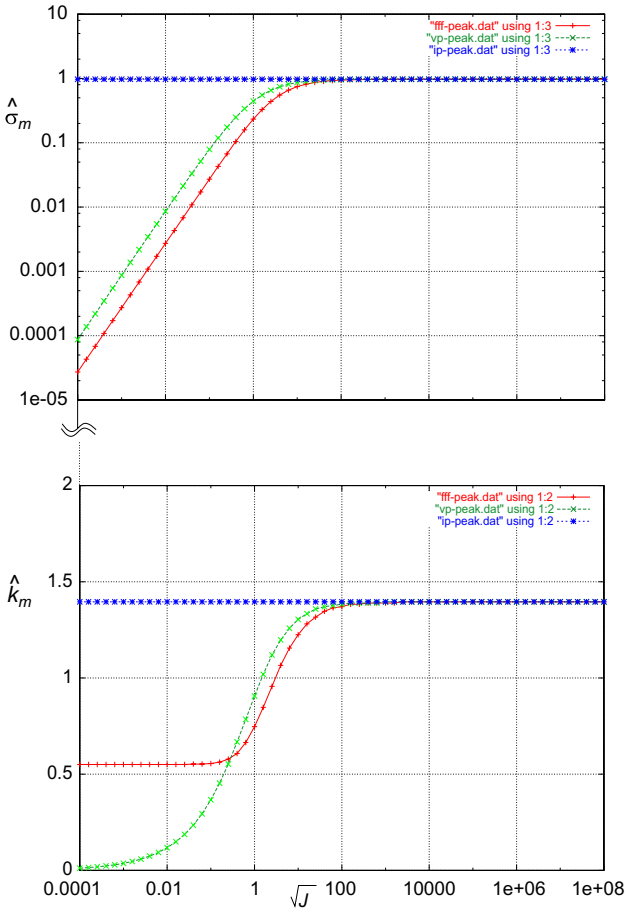

Figure 8.5: $\hat{\sigma}_m$ *and* $\hat{k}_m$ *vs.* $\sqrt{J}$ *for values of* ℓ *and* m *for Water and air.*

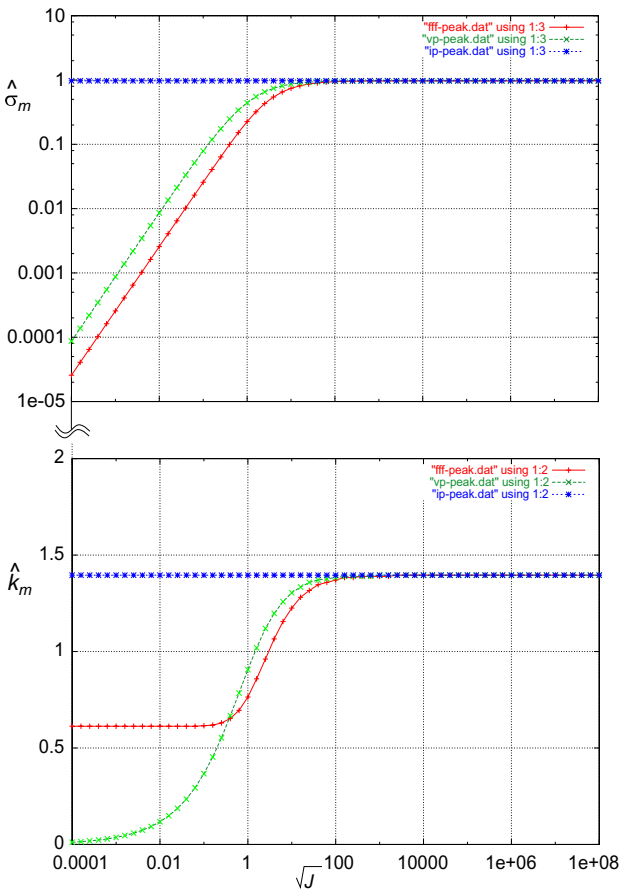

Figure 8.6: $\hat{\sigma}_m$ *and* $\hat{k}_m$ *vs.* $\sqrt{J}$ *for values of* ℓ *and* m *for Benzene and air.*

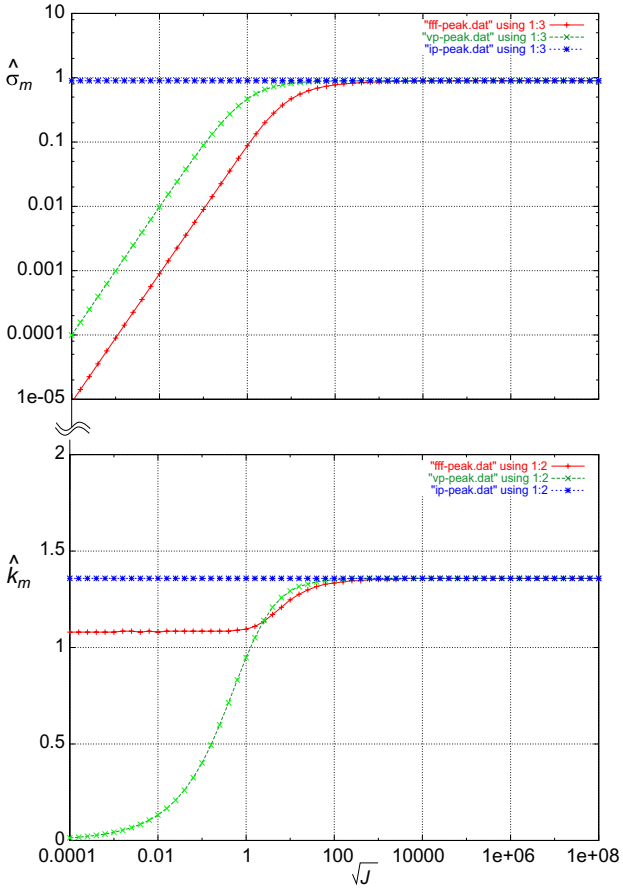

Figure 8.7: $\hat{\sigma}_m$ *and* $\hat{k}_m$ *vs.* $\sqrt{J}$ *for values of* ℓ *and* m *for Water and Benzene.*

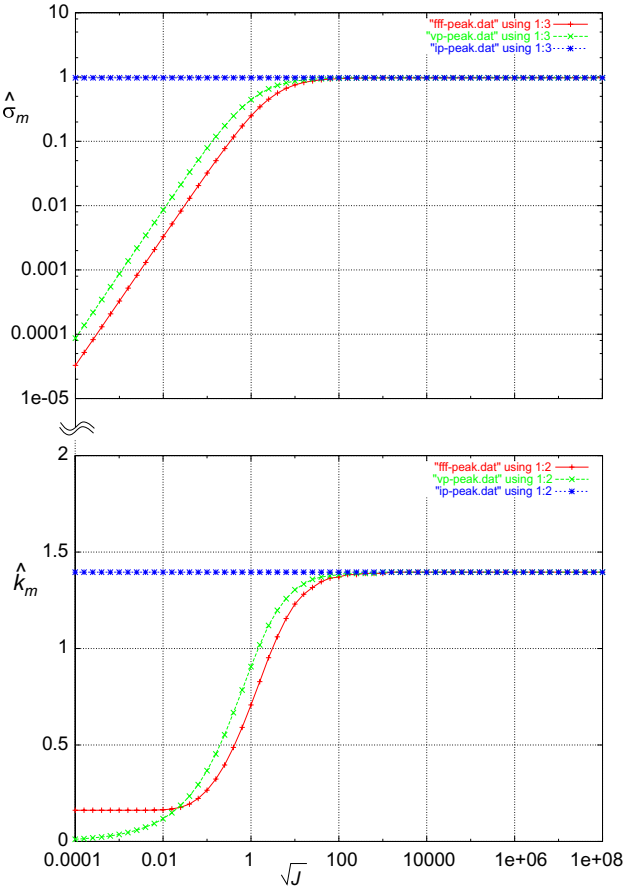

Figure 8.8: $\hat{\sigma}_m$ *and* $\hat{k}_m$ *vs.* $\sqrt{J}$ *for values of* ℓ *and* m *for SO100 and air.*

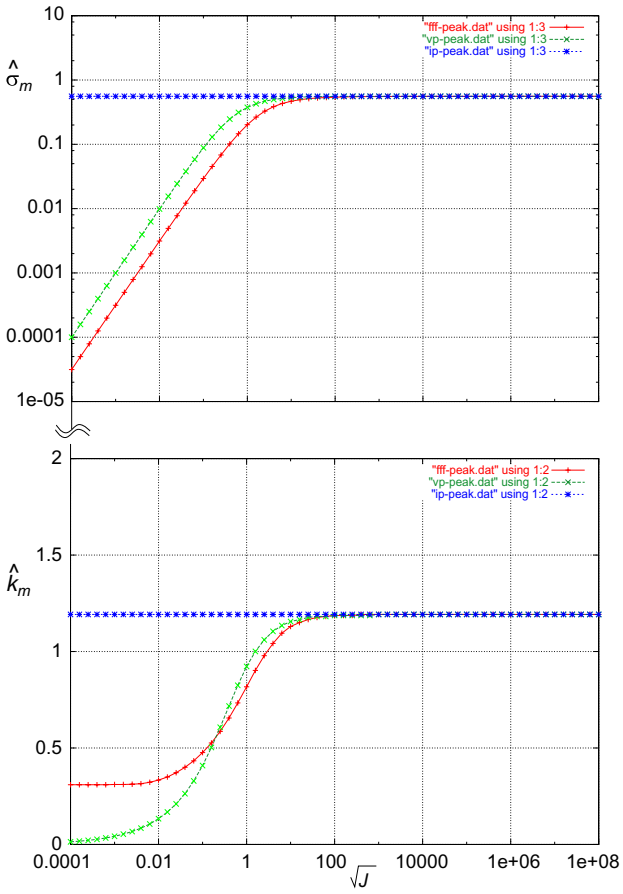

Figure 8.9: $\hat{\sigma}_m$ *and* $\hat{k}_m$ *vs.* $\sqrt{J}$ *for values of* ℓ *and* m *for glycerine and mercury.*

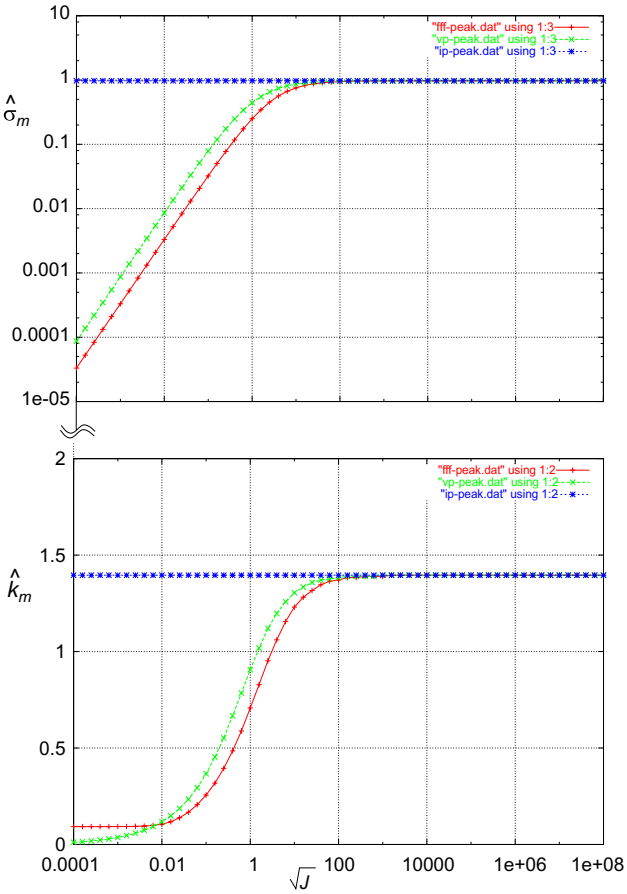

Figure 8.10: $\hat{\sigma}_m$ *and* $\hat{k}_m$ *vs.* $\sqrt{J}$ *for values of* ℓ *and* m *for glycerine and air.*

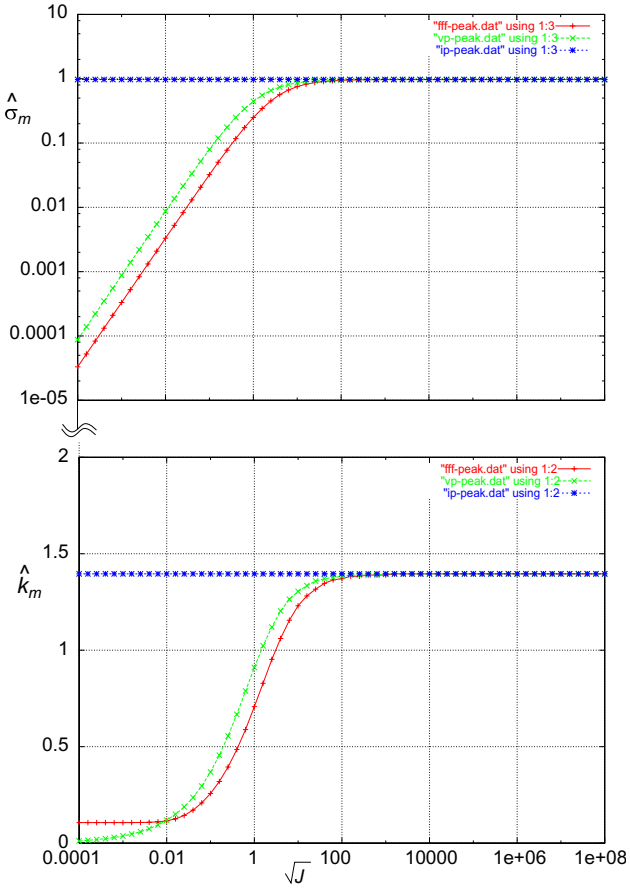

Figure 8.11: $\hat{\sigma}_m$ *and* $\hat{k}_m$ *vs.* $\sqrt{J}$ *for values of* ℓ *and* m *for oil and air.*

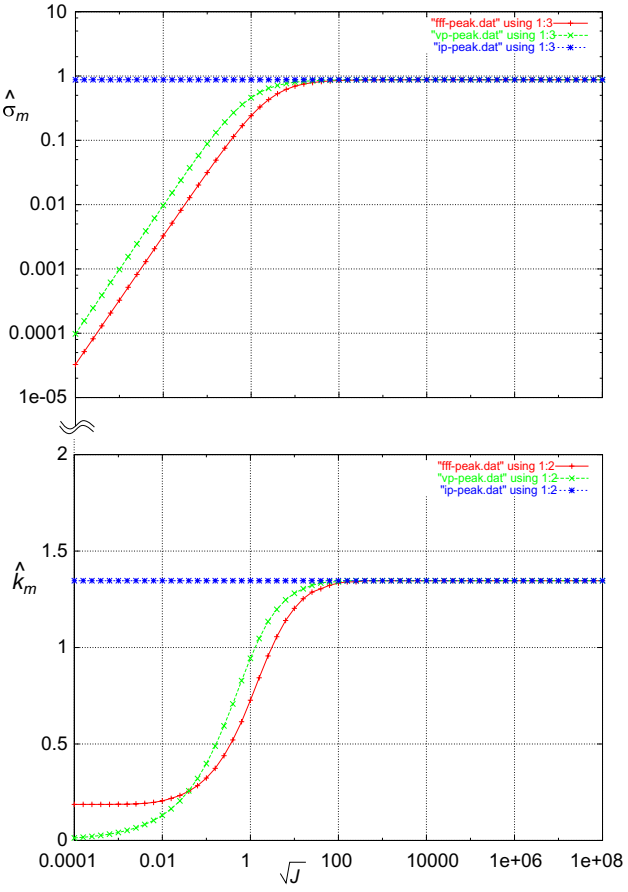

Figure 8.12: $\hat{\sigma}_m$ *and* $\hat{k}_m$ *vs.* $\sqrt{J}$ *for values of* ℓ *and* m *for goldensyrup and paraffin.*

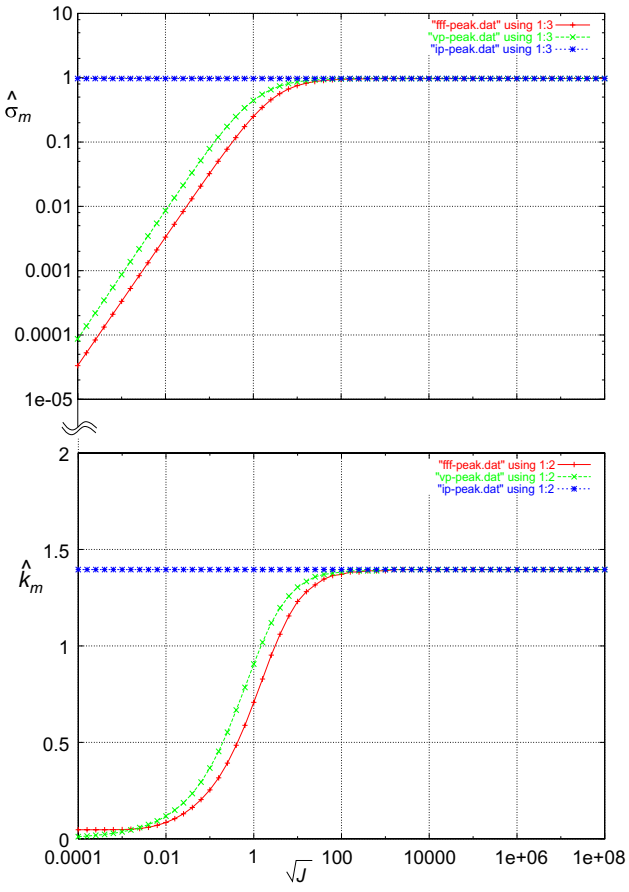

Figure 8.13: $\hat{\sigma}_m$ *and* $\hat{k}_m$ *vs.* $\sqrt{J}$ *for values of* ℓ *and* m *for SO10000 and air.*

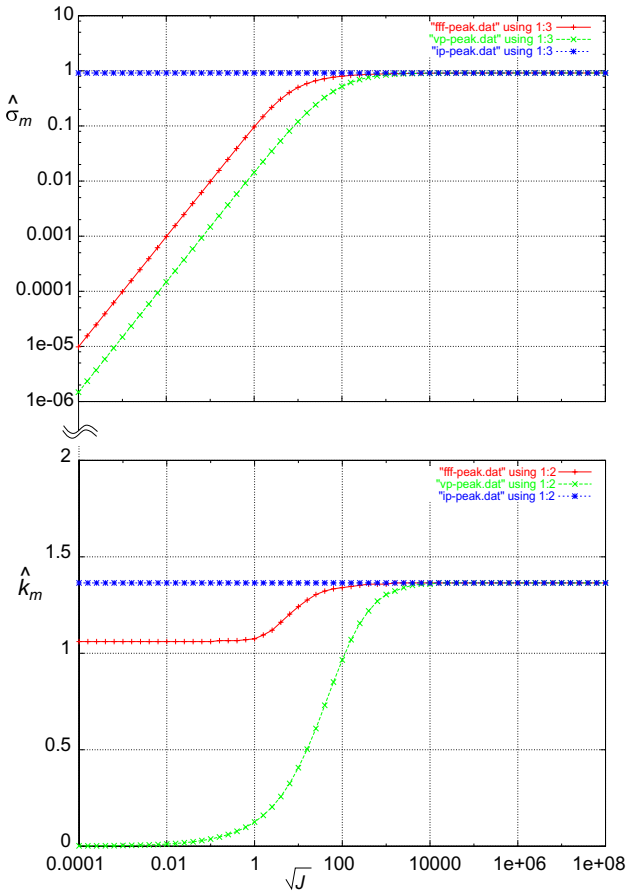

Figure 8.14: $\hat{\sigma}_m$ *and* $\hat{k}_m$ *vs.* $\sqrt{J}$ *for values of* ℓ *and* m *for goldensyrup and BB oil.*

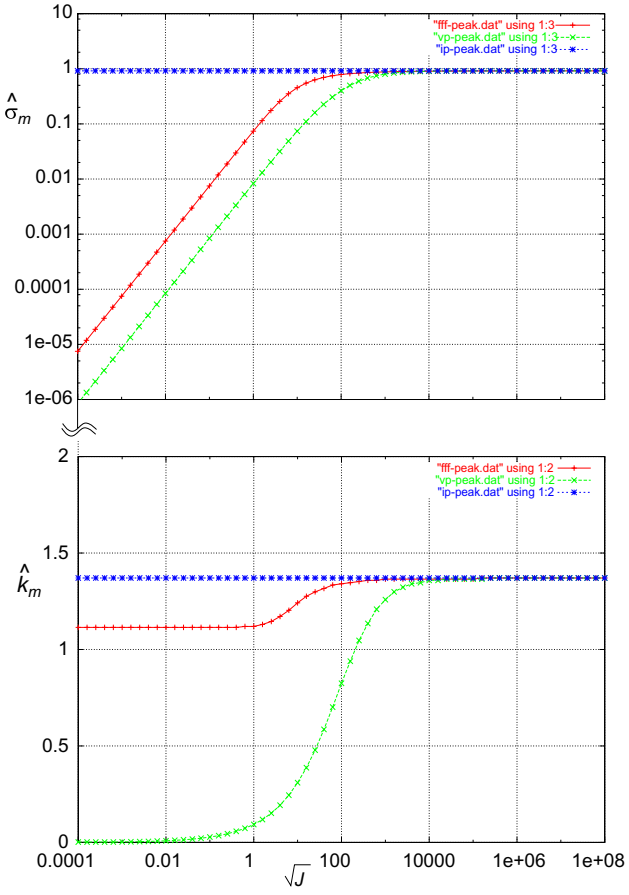

Figure 8.15: $\hat{\sigma}_m$ *and* $\hat{k}_m$ *vs.* $\sqrt{J}$ *for values of* ℓ *and* m *for goldensyrup and black lubrication oil.*

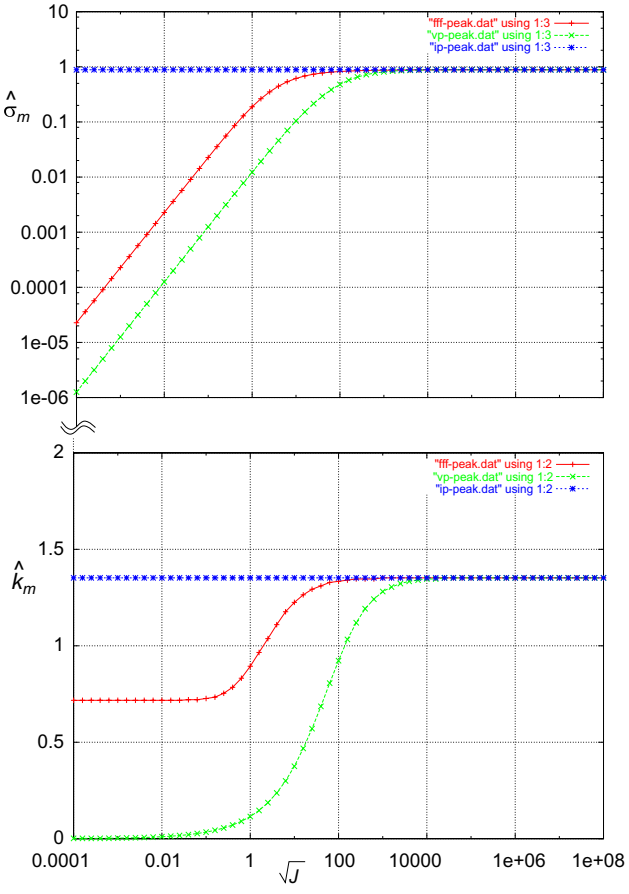

Figure 8.16: $\hat{\sigma}_m$ *and* $\hat{k}_m$ *vs.* $\sqrt{J}$ *for values of* ℓ *and* m *for Tar pitch mixture and Goldensyrup.*

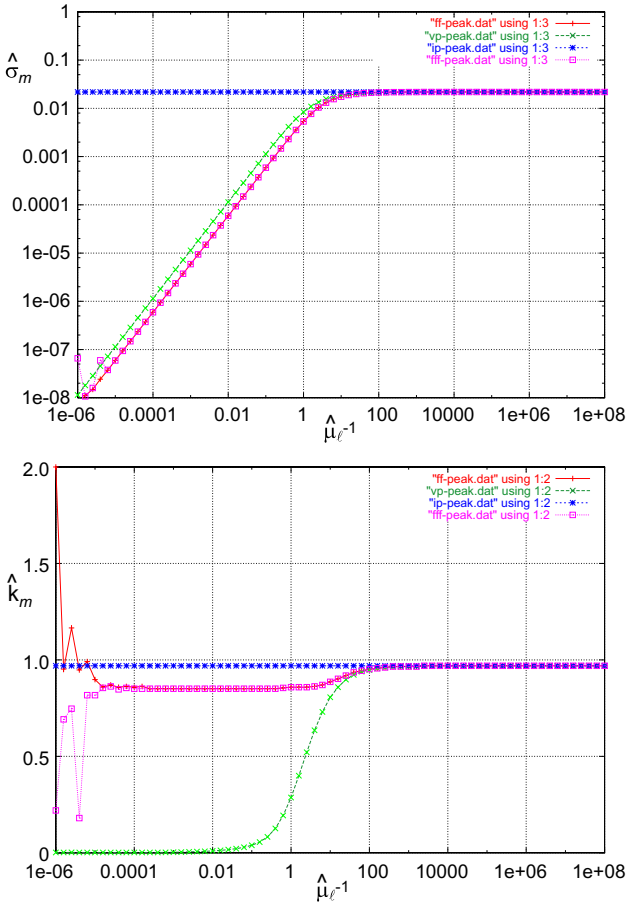

Figure 8.17: $\hat{\sigma}_m$ *and* $\hat{k}_m$ *vs.* $\sqrt{J}$ *for values of* ℓ *and* m *for mercury and air.*

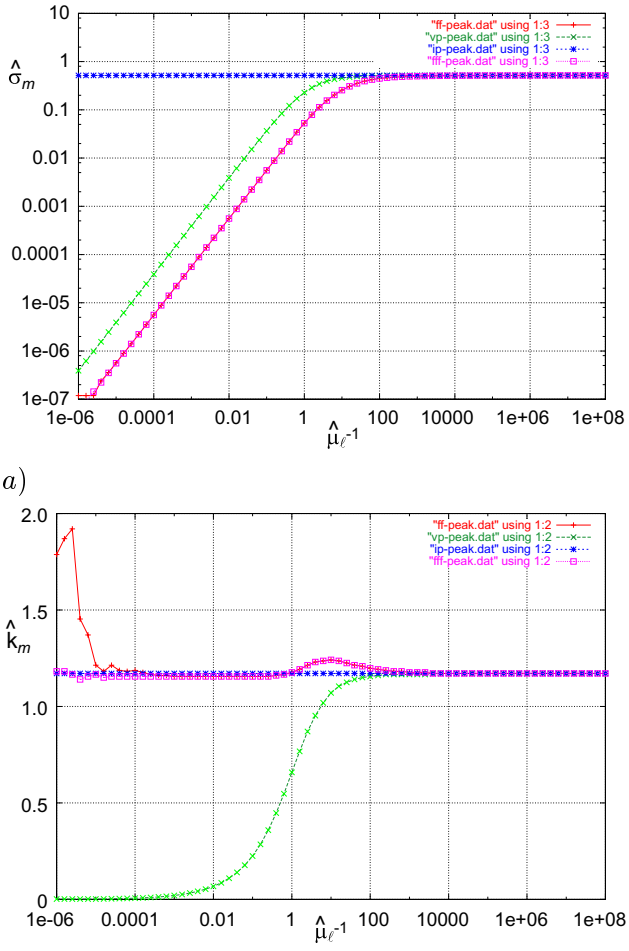

$a)$

Figure 8.18: $\hat{\sigma}_m$ *and* $\hat{k}_m$ *vs.* $\sqrt{J}$ *for values of* ℓ *and* m *for mercury and water.*

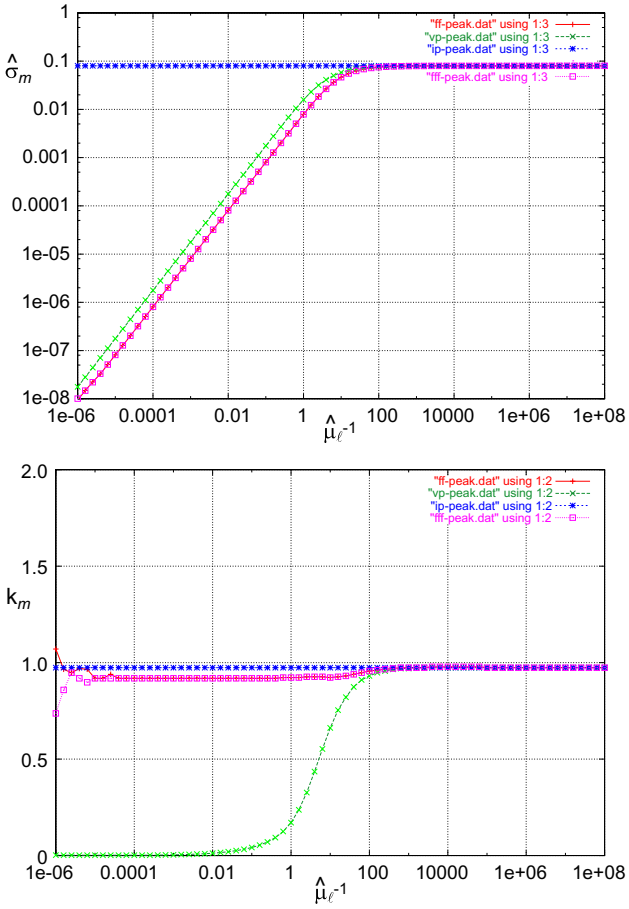

Figure 8.19: $\hat{\sigma}_m$ *and* $\hat{k}_m$ *vs.* $\sqrt{J}$ *for values of* ℓ *and* m *for Water and air.*

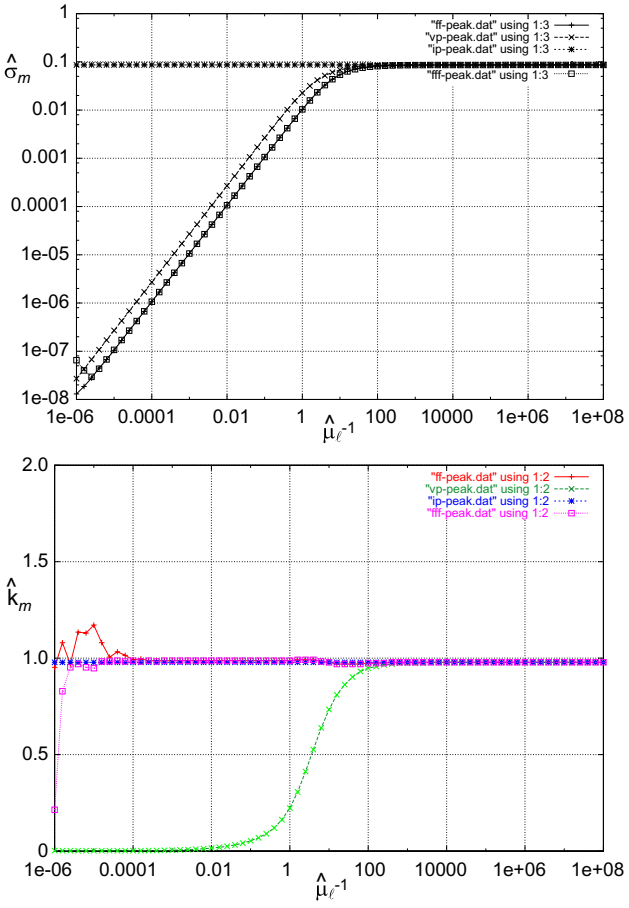

Figure 8.20: $\hat{\sigma}_m$ *and* $\hat{k}_m$ *vs.* $\sqrt{J}$ *for values of* ℓ *and* m *for Benzene and air.*

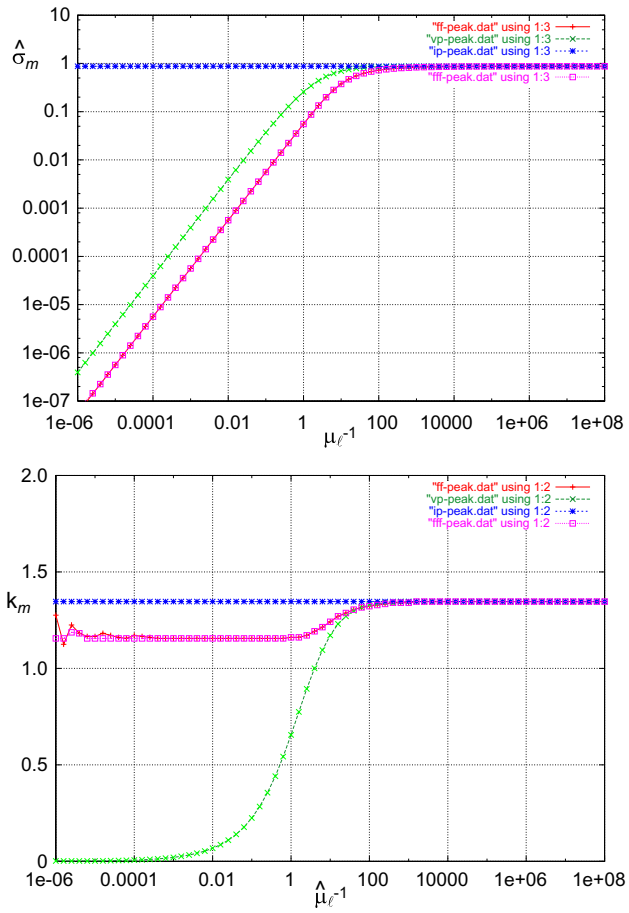

Figure 8.21: $\hat{\sigma}_m$ *and* $\hat{k}_m$ *vs.* $\sqrt{J}$ *for values of* ℓ *and* m *for Water and Benzene.*

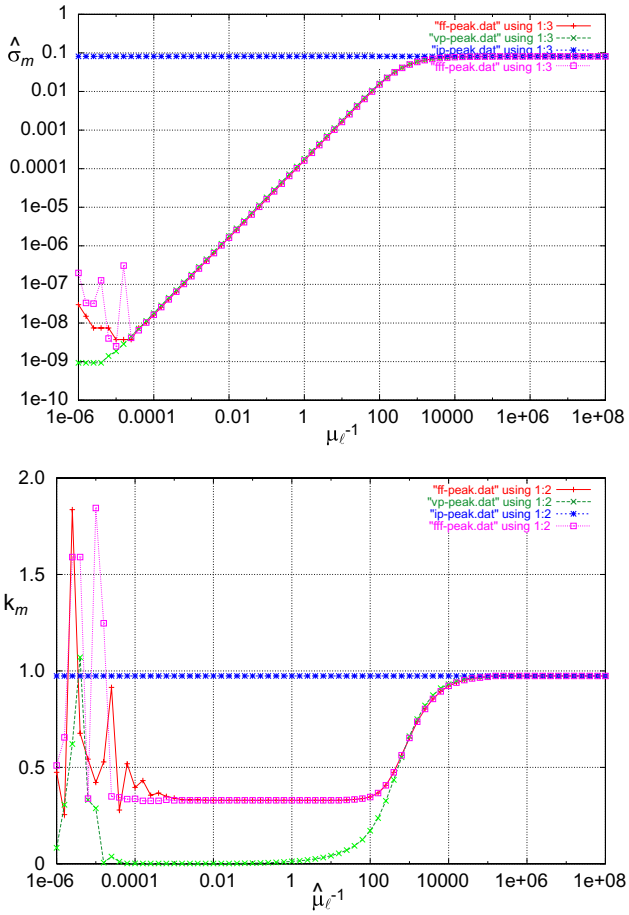

Figure 8.22: $\hat{\sigma}_m$ *and* $\hat{k}_m$ *vs.* $\sqrt{J}$ *for values of* ℓ *and* m *for SO100 and air.*

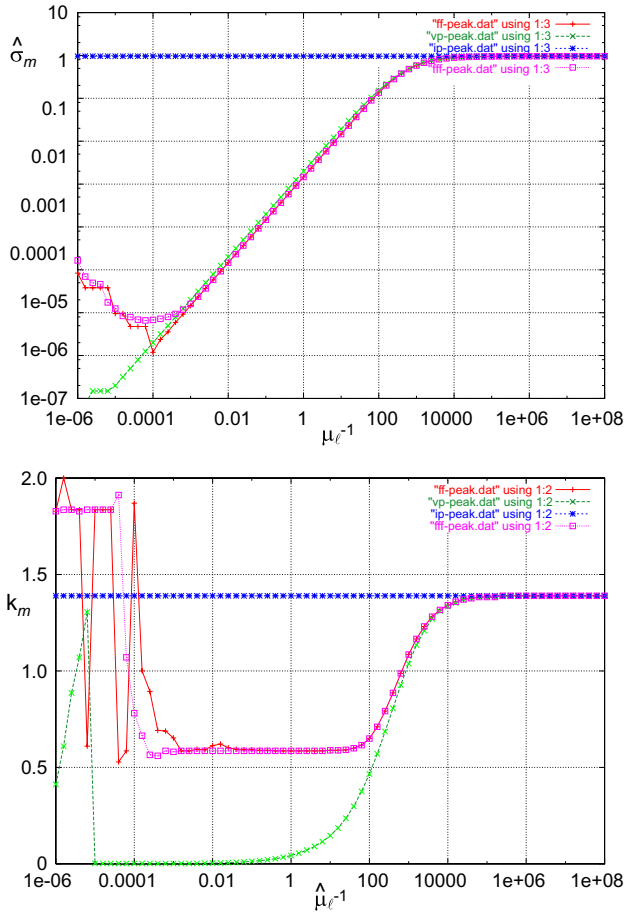

Figure 8.23: $\hat{\sigma}_m$ *and* $\hat{k}_m$ *vs.* $\sqrt{J}$ *for values of* ℓ *and* m *for glycerine and mercury .*

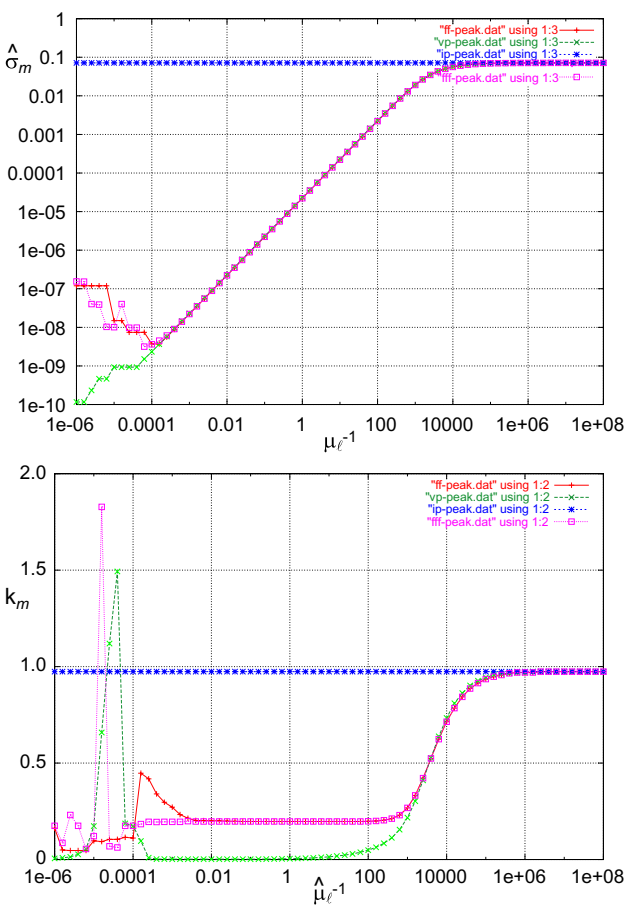

Figure 8.24: $\hat{\sigma}_m$ *and* $\hat{k}_m$ *vs.* $\sqrt{J}$ *for values of* ℓ *and* m *for glycerine and air.*

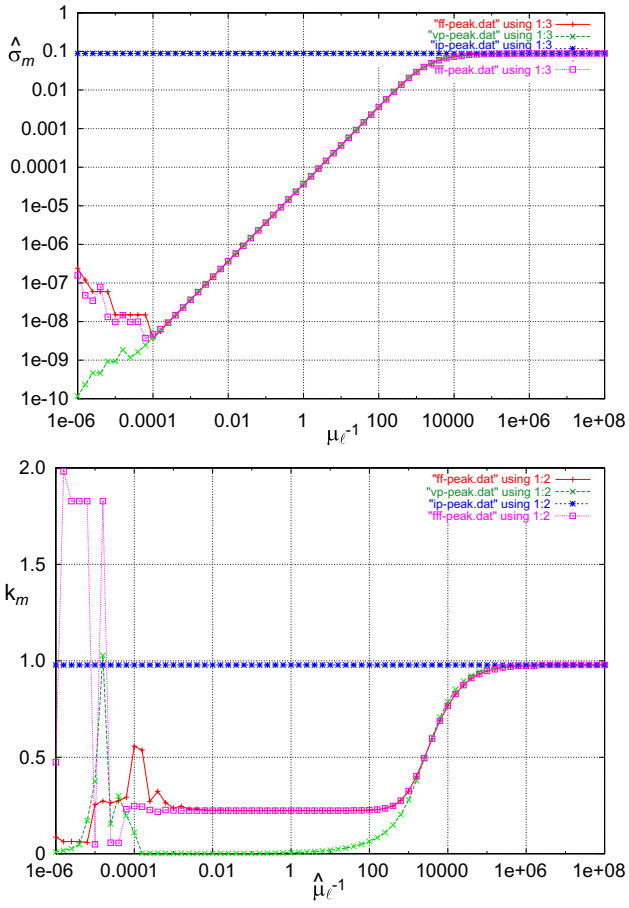

Figure 8.25: $\hat{\sigma}_m$ *and* $\hat{k}_m$ *vs.* $\sqrt{J}$ *for values of* ℓ *and* m *for oil and air.*

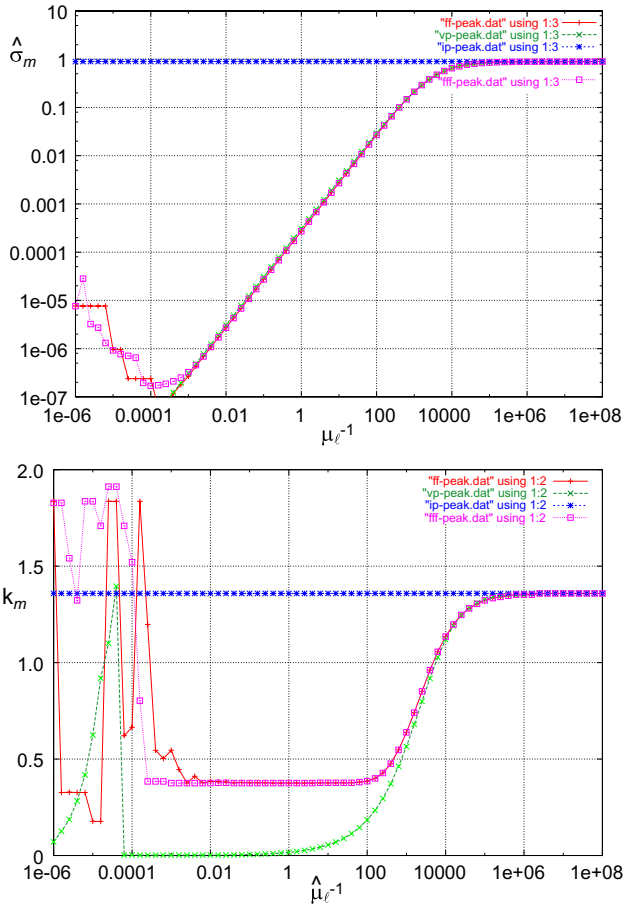

Figure 8.26: $\hat{\sigma}_m$ *and* $\hat{k}_m$ *vs.* $\sqrt{J}$ *for values of* ℓ *and* m *for goldensyrup and paraffin.*

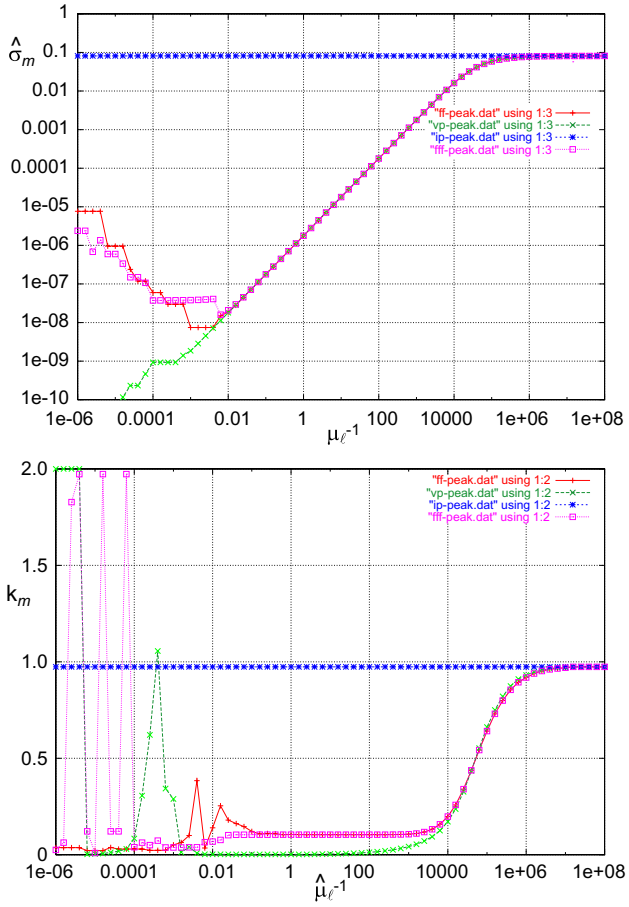

Figure 8.27: $\hat{\sigma}_m$ *and* $\hat{k}_m$ *vs.* $\sqrt{J}$ *for values of* ℓ *and* m *for SO10000 and air.*

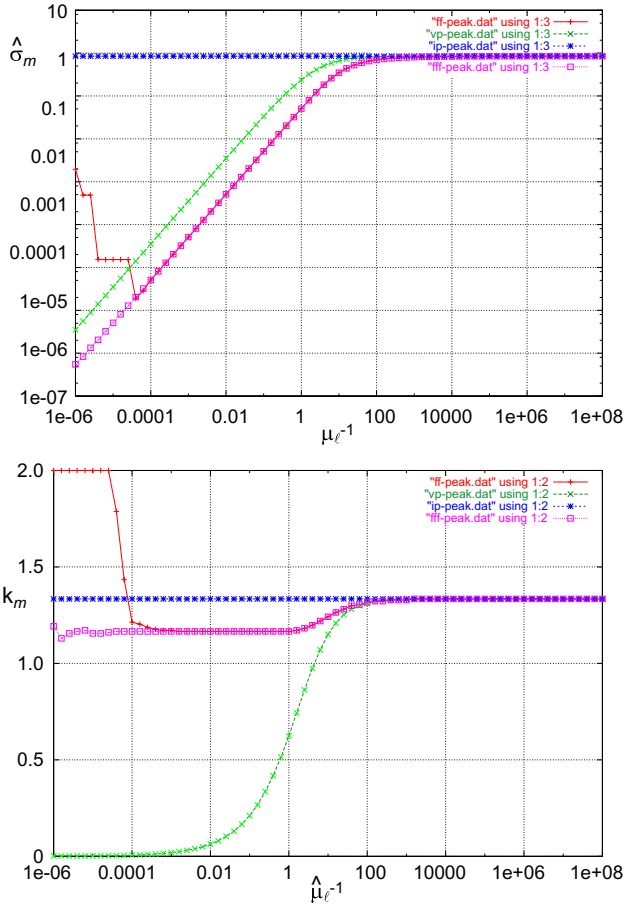

Figure 8.28: $\hat{\sigma}_m$ *and* $\hat{k}_m$ *vs.* $\sqrt{J}$ *for values of* ℓ *and* m *for goldensyrup and BB oil.*

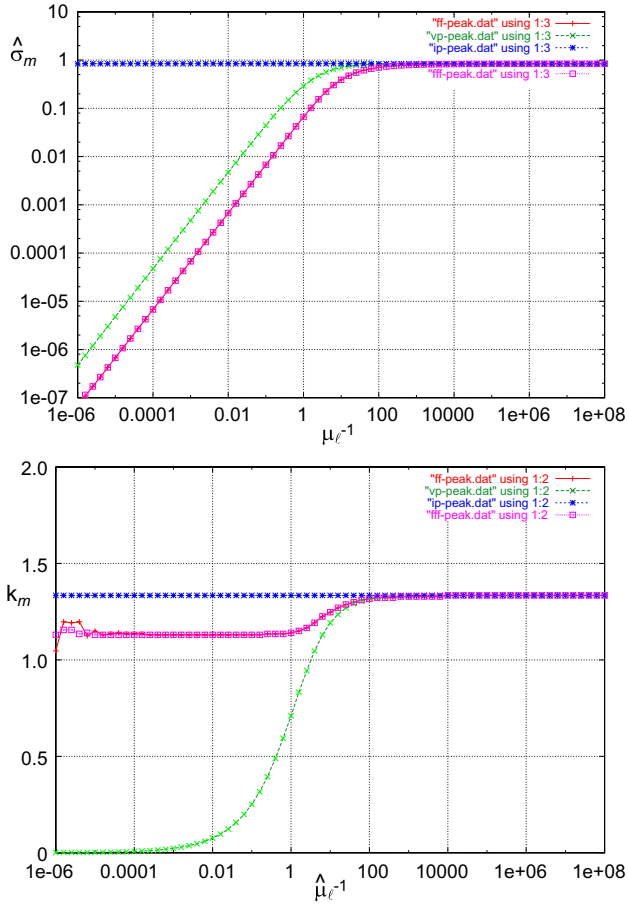

Figure 8.29: $\hat{\sigma}_m$ *and* $\hat{k}_m$ *vs.* $\sqrt{J}$ *for values of* ℓ *and* m *for goldensyrup and black lubrication oil.*

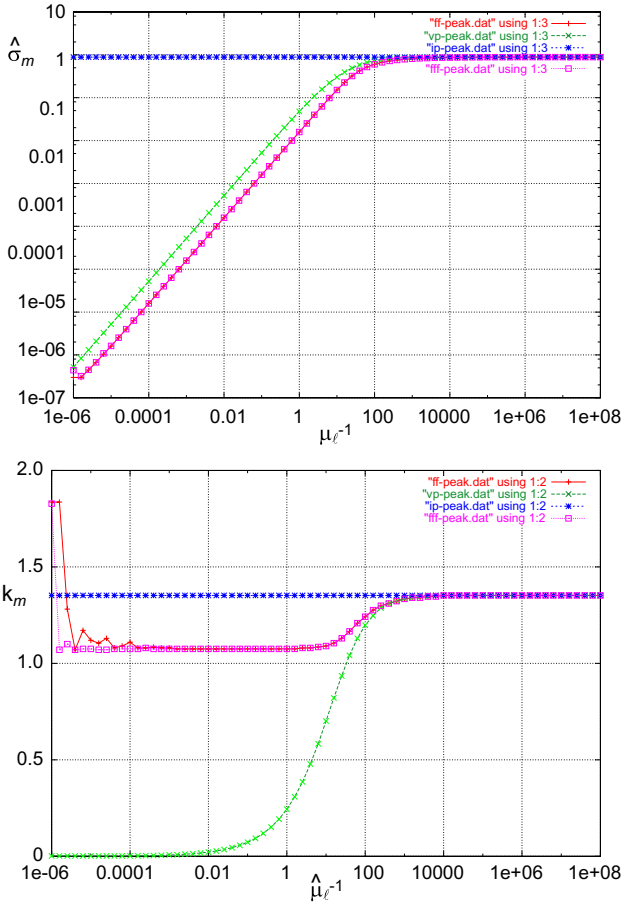

Figure 8.30: $\hat{\sigma}_m$ *and* $\hat{k}_m$ *vs.* $\sqrt{J}$ *for values of* ℓ *and* m *for Tar pitch mixture and Goldensyrup.*

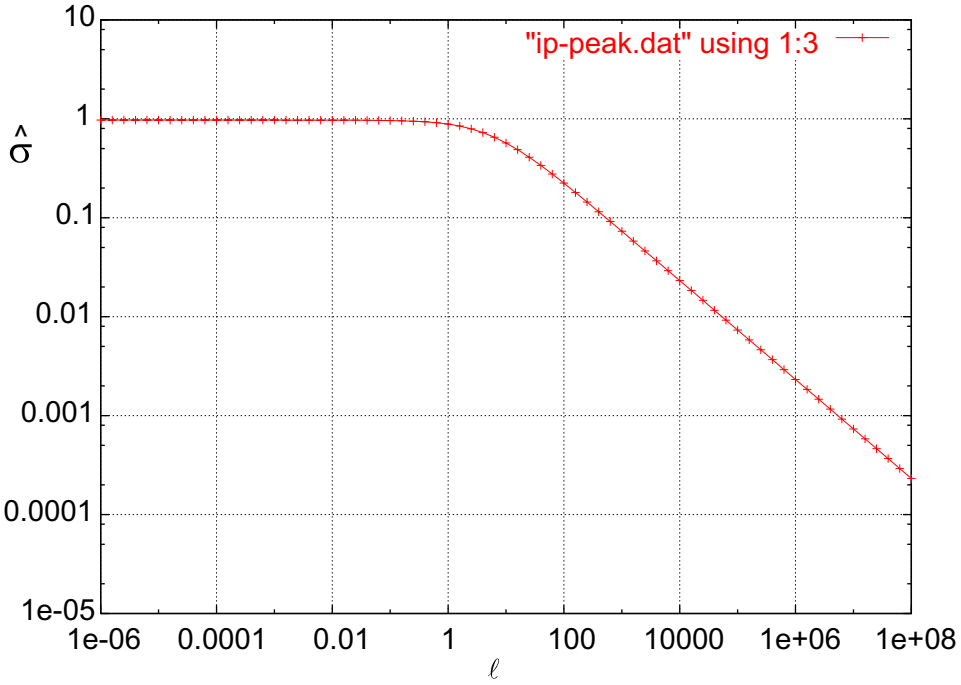

Figure 8.31: *Maximum growth rate according to inviscid theory as a function of the density ratio. For values of ℓ more than 100, the growth rate decreases with increasing ℓ.*

The asymptotic flat values of $\hat{\sigma_m}$ and $\hat{k}_m$ for large values of the Reynolds number J correspond to an inviscid limit. However, this limit cannot depend on viscosity so that dependence on m in evidence in figure 8.1 is an artifact of the way $\hat{\sigma}$ is made dimensionless with $T = \mu d/\gamma$. If instead of $V = \gamma/\mu$ we use $T = D/U$ with $U = \sqrt{\gamma/D\rho}$ then $\hat{\sigma}$ does not depend on μ, m or J. The variation $\hat{\sigma_m}$ and $\hat{k}_m$ with ℓ for IPF is exhibited in figures 8.31 and 8.32.

9 Conclusions and discussion

We studied capillary instability of a fluid cylinder of viscosity μ_ℓ in a fluid with viscosity μ_a; the fluids may be liquid or gas. The problem is completely characterized by three numbers: a viscosity ratio $m = \mu_a/\mu_\ell$, a density ratio $\ell = \rho_a/\rho_\ell$ and by a Reynolds number $J = \rho\gamma D/\mu^2$ based on a collapse velocity γ/μ where μ and ρ are for the more viscous of the two fluids. The goal of the present study is to evaluate the utility of viscous potential flow as an approximation to the unapproximated viscous problem introduced by Tomotika (1935) and studied for special cases by Chandrasekhar (1961) and for limiting cases by Lee and Flumerfelt (1981). The effects of vorticity and the continuity of the tangential compoenent of velocity and stress cannot be enforced in the frame of potential flow of a viscous fluid, but the extensional effects of viscous stresses on capillary collapse are retained in the normal stress balance.

We found that inviscid potential flow emerges as a unique high Reynolds limit (practically, with $J > O(10)$ of both the fully viscous and viscous potential flow analysis. The inviscid limit depends only on the density ratio ℓ; analysis shows that the dimensionless growth rate is nearly constant when $\ell < 1$ and decreases linearly with ℓ for $\ell > 1$, whereas the associated dimensionless wavenumber decreases from a value of 1.4 to a value slightly less than one as ℓ decreases from about 1 to 100 (figures 8.1 and 8.2).

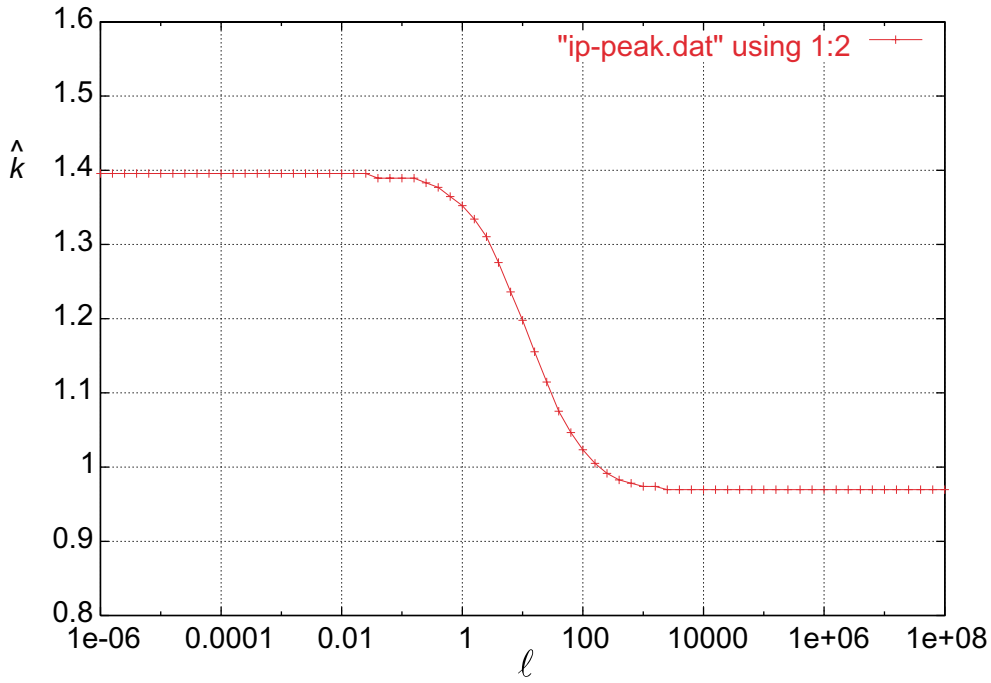

Figure 8.32: *Wavenumber for maximum growth (figure 8.1) vs. ℓ. The maximum values are not sensitive to $\ell = \rho_a/\rho_\ell$ where ℓ is small.*

Analysis of the viscous flow reveals the existence of finite minimum and finite maximum values of $\hat{k}_m$, for certain viscosity ratios, as J is increased (figures 8.1 and 8.2.

Comparisons of growth rate curves in dimensions for fully viscous flow, viscous potential flow and inviscid potential flow are given in figures 7.1–7.28 for 28 fluid pairs. Comparisons of the maximum dimensional growth rate $\hat{\sigma_m}$ and associated wavenumber $\hat{k}_m$ as a function of $\sqrt{J}$ for different values of m and ℓ are presented in figures 8.3–8.30. From these figures we may conclude that the maximum growth rates and wavenumber for inviscid potential flow, viscous potential flow and fully viscous flow converge when J is large; for smaller J, the growth rates of inviscid potential flow are greatest (and independent of J) and these fully viscous flow are smallest and decrease with decreasing J. The growth rates of viscous potential flow flow track fully viscous flow and lie between inviscid potential flow and fully viscous flow. A similar behavior is exhibited by the associated wavenumbers, with viscous potential flow giving the $\hat{k}_m$ and inviscid potential flow the largest $\hat{k}_m$ when $\sqrt{J}$ is not too large.

It follows from the comparisons just presented, that viscous potential flow is a much better approximation of fully viscous flow than inviscid potential flow for small J and no worse than inviscid potential flow for all J. There is absolutely no advantage to putting the viscosities to zero in the analysis of potential flow.

The convergence of fully viscous flow and viscous potential flow to inviscid potential flow when the Reynolds number J is large could have been anticipated from general fluid mechanical principles. On the other hand, Harper (1972) has argued (see also Joseph and Liao 1994, pp 6 and 7) that the success of the Levich (1949,1962) [6] potential flow approximation in calculating the drag on a rising spherical bubble of gas is due to the nature of the boundary layer at a tangentially stress-free surface. Presumably liquid-gas surfaces approximate such stress free conditions when the viscosity contrast is large, but not at liquid-liquid surfaces like water and benzene in which the viscosities are comparable.

Levich computed the drag by equating UD, where U is the rise velocity and D the drag, to the viscous

dissipation in the liquid as would be true for the steady drag on a solid. The approximation arises on both sides of the balance, on the left side by assuming that every part of the boundary of the bubble moves with the same velocity U, and on the right, by evaluating the dissipation integral on potential flow over a sphere.

Our calculations of capillary instability given here show that viscous potential flows approximate fully viscous liquid-liquid as well as gas-liquid flows in cases in which inviscid potential flow fails dismally provided only that J is not too small.

Acknowledgement This work was supported by the NSF/CTS-0076648, the Engineering Research Program of the Office of Basic Energy Sciences at the DOE and by an ARO grant DA/DAAH04.

References

[1] Chandrasekhar, S. 1961. Hydrodynamic and Hydromagnetic Stability. Oxford Univ. Press.

[2] Funada, T & Joseph, D.D., 2001. Viscous potential flow analysis of Kelvin-Helmholtz instability in a channel, accepted *J. Fluid Mech.*

[3] Harper, J.F. 1972. The motion of bubbles and drops through liquids, *Adv. Appl. Mech.* **12** 59-129.

[4] Joseph, D.D., Belanger, J. & Beavers, G.S. 1999. Breakup of a liquid drop suddenly exposed to a high-speed airstream, *Int. J. Multiphase Flow* **25**, 1263-1303.

[5] Joseph, D.D. & Liao, T.Y. 1994. Potential flows of viscous and viscoelastic fluids, *J. Fluid Mech.*, **265**, 1-23.

[6] Levich, V.G. 1949. The motion of bubbles at high Reynolds numbers. *Zh. Eksperim Teor. Fiz.* **19**, 18; also see *Physiochemical Hydrodynamics*, English translation by Scripta Technica, Prentice-Hall, Englewood Cliffs, NJ, 1962, p. 436ff.

[7] Lee, W.K. & Flumerfelt, R.W. 1981. Instability of stationary and uniformly moving cylinderical fluid bodies-I. Newtonian systems *Int. J. Multiphase Flow*, **7**(2), 363-381.

[8] Plateau, 1873. *Statique experimentale et theorique des liquide soumis aux seules forces moleculaire*, **vol ii**, 231.

[9] Rayleigh, Lord, 1879. On the capillary phenomena of jets, *Proc. Roy. Soc. London A*, **29**, 71-79.

[10] Rayleigh, Lord, 1892. On the instability of a cylinder of viscous liquid under capillary force, *Phil. Mag*, **34**(207), 145-154.

[11] Tomotika, S., 1935. On the instability of a cylindrical thread of a viscous liquid surrounded by another viscous fluid, *Proc. Roy. Soc. London A*, **150**, 322-337.

[12] Weber, C., 1931. Zum Zerfall eines Flüssigkeitsstrahles. Ztschr. f. angew. *Math. und Mech.*, **11**(2), 136-154.